LAYER-BY-LAYER ASSEMBLY OF POLY(3,4-ETHYLENEDIOXYTHIOPHENE) THIN FILMS: TAILORING GROWTH AND UV-PROTECTION

A Thesis

by

THOMAS JAMES DAWIDCZYK

Submitted to the Office of Graduate Studies of
Texas A&M University
in partial fulfillment of the requirements for the degree of

MASTER OF SCIENCE

May 2008

Major Subject: Mechanical Engineering

LAYER-BY-LAYER ASSEMBLY OF POLY(3,4-ETHYLENEDIOXYTHIOPHENE) THIN FILMS: TAILORING GROWTH AND UV-PROTECTION

A Thesis

by

THOMAS JAMES DAWIDCZYK

Submitted to the Office of Graduate Studies of
Texas A&M University
in partial fulfillment of the requirements for the degree of

MASTER OF SCIENCE

Approved by:

Chair of Committee,	Jaime Grunlan
Committee Members,	Xinghang Zhang
	Michael McShane
Head of Department,	Dennis O'Neal

May 2008

Major Subject: Mechanical Engineering

ABSTRACT

Layer-by-Layer Assembly of Poly(3,4-Ethylenedioxythiophene) Thin Films: Tailoring Growth and UV-Protection. (May 2008)

Thomas James Dawidczyk, B.S., The University of Massachusetts at Amherst

Chair of Advisory Committee: Dr. Jaime Grunlan

Conductive thin films of poly(3,4-ethylenedioxythiophene)-polystyrenesulfonate (PEDOT-PSS) were created via layer-by-layer assembly. The PEDOT-PSS was used in an aqueous solution as an anionic polyelectrolyte, with both linear and branched polyethylenimine (PEI) and poly(allylamine hydrochloride) (PAH) in the positive aqueous solution. The electrical conductivity was varied by altering pH, concentration, polyelectrolyte, and doping the PEDOT with dimethylsulfoxide (DMSO). The most conductive 12BL samples were doped with 1wt% DMSO and have a sheet resistance of approximately 8kΩ/□. Despite exhibiting good initial conductivity, these PEDOT based thin films degrade under ultraviolet (UV) exposure.

UV absorbing nanoparticles were added into the cationic solution in an effort to reduce UV sensitivity. The final bilayers of the films contained either colloidal titanium dioxide (TiO_2) or carbon black (CB) and the films were exposed to a 365nm UV-light with an intensity of 2.16mW/cm^2 for 9 days. The UV light at this intensity correlates to approximately four years of sunlight. The initial sheet resistances for all samples were similar, but the UV-degradation was reduced by a factor of 5 by utilizing TiO_2 and CB in

the final bilayers. In addition to being the most conductive after UV exposure, the TiO_2 containing film was also 27% more optically transparent than the pure PEDOT films. These additional UV-absorbing nanoparticles extend the operational life of the PEDOT films and, in the case of TiO_2, do so without any reduced transparency.

DEDICATION

To my family

ACKNOWLEDGEMENTS

I would like to thank my mother, father, and rest of my family for encouraging me to return to graduate school and their continued support throughout my graduate degree.

I thank my committee chair, Dr. Jaime Grunlan, for his support and guidance during my time at Texas A&M University and would also like to thank Dr. Zhang and Dr. McShane for being supportive members of my committee.

Thanks also go to my friends and colleagues, research associates, and the Mechanical Engineering Department faculty and staff for making my time at Texas A&M University a wonderful experience.

TABLE OF CONTENTS

LIST OF FIGURES

FIGURE Page

FIGURE Page

LIST OF TABLES

CHAPTER I

INTRODUCTION

The layer-by-layer (LbL) assembly technique is a popular method used to create functional thin films that are generally less than one micrometer thick.[1-3] Films are typically made by alternately depositing positively and negatively charged species via dilute aqueous solutions, as shown in Figure 1. The ability to finely tune various properties by changing processing variables makes LbL applicable to a broad range of applications. Antimicrobial,[4-6] biocompatible,[7-9] electrically conductive,[10,11] electrochromic,[12,13] and anti-reflective[14,15] films have all been prepared using LbL assembly. In the present study poly(3,4-ethylenedioxythiophene), an intrinsically conductive polymer, has been used to create tunable electrically conductive films.

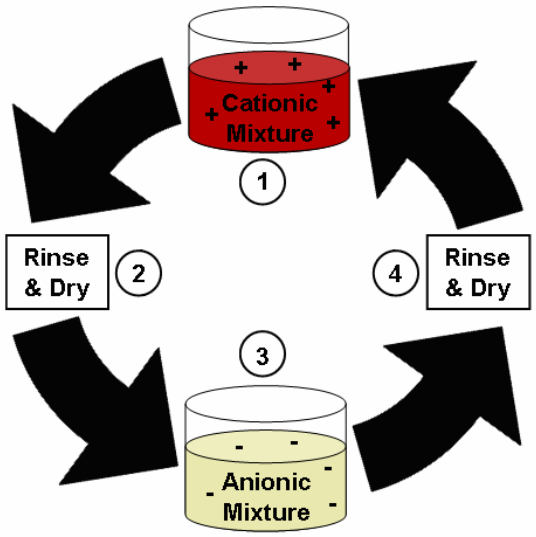

Figure 1. Schematic of the layer-by-layer assembly process.

The thesis follows the style of *Langmuir*.

Langmuir and Blodgett first introduced a technique for layered assembly in the 1920's that served as a precursor for LbL assembly. Amphiphilic monolayers on the surface of water were transferred to a substrate by dipping the substrate into the solution[16] To achieve multiple layers, the substrate was simply dipped multiple times. The thickness of the film is determined by the number of dips and the size of the molecule being used.[17] The drawback to the Langmuir-Blodgett technique is that the films are generally thermally and structurally unstable and there are limited materials that combine the necessary properties of organic solubility, shear resistance and cohesion, stability at the subphase surface, proper orientation and compaction.

Decher and coworkers developed a more practical method for self assembly,[2] building upon the early work of Iler who focused exclusively on inorganic particles.[18] Films were made utilizing the electrostatic attraction between oppositely charged polyelectrolytes resulting in uniform thickness and deposition.[3] The benefit over the Langmuir-Blodgett technique is that absorption process is independent of the substrate size and topology,[17] the layers can be varied without changing the process, the thickness can be controlled down to the nano-level and the films can be processed under ambient conditions.

The modern layer-by-layer assembly process is characterized by alternately depositing oppositely charged species via dilute aqueous solutions, but uncharged species with other mutual attractions have also been used.[19] A charged or polar substrate is submerged into an oppositely charged polyelectrolyte solution for a

given time. The polyelectrolytes are attracted to the surface until a charge inversion develops which repels further growth.[20] The substrate is removed, rinsed and dried, and then submerged into the alternate electrolyte solution. Figure 1 schematically depicts the LbL deposition process. Each deposited cationic/anionic pair is referred to as a bilayer. The thickness of each bilayer is typically 1-100+ nm thick[21] and can be tailored by altering the pH,[22] counter ion,[23] ionic strength,[24] chemistry,[25] molecular weight,[26] and temperature.[27] Figure 2 illustrates how the layers build upon a substrate. Bilayer growth can be either linear or exponential depending on the strength of charge in the layers, with weaker charge leading to more exponential growth.[28-30]

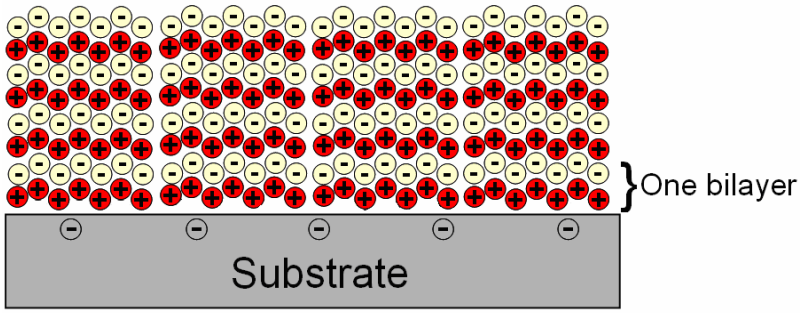

Figure 2. Schematic of a layer-by-layer thin film assembled on a substrate.

Nanoparticles can be added to the deposition mixtures along with the polyelectrolyte, which provides for additional functionality of the film.[31] Single wall carbon nanotubes (SWMTs) were deposited to enhance thin film mechanical strength and thermal stability.[32] To make the SWNTs water soluble, either the side walls were covalently functionalized or a surfactant was added. Titania filled nanocomposite films for UV protection were made with titania nanoparticles[33] and

nanosheets[34] dispersed with a polyelectrolyte. Easily manipulable, M13 Viruses were used in conjunction with linear polyethylenimine (LPEI) to make biocompatible films.[9] GaN was added to these films to make them fluoresce, allowing for a variety of sensor applications. Actuators were made by adding platinum nanoclusters to LbL films deposited on an electrically conductive substrate and applying a voltage.[35] Figure 3 highlights some of these functionalities.

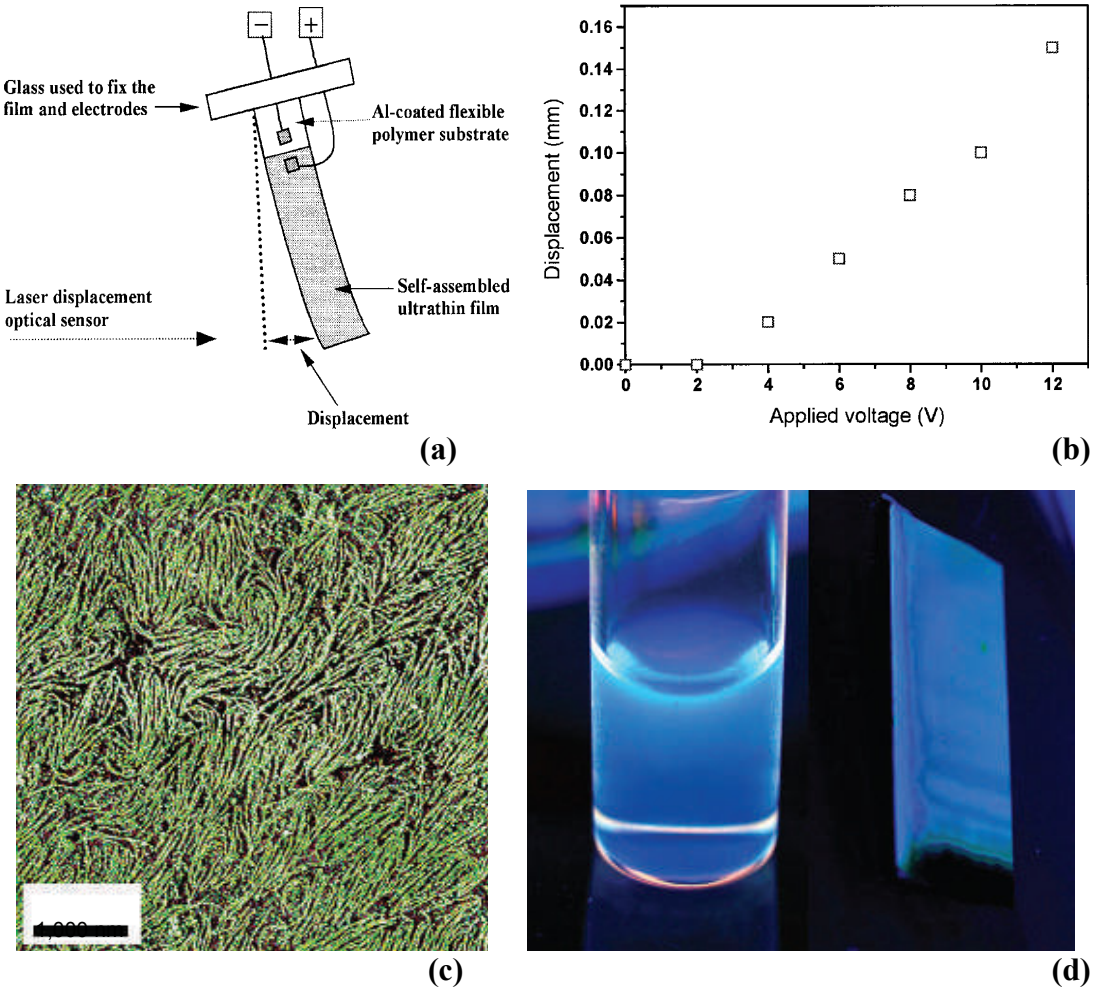

Figure 3. Schematic of the LbL actuator (a) with the displacement per applied voltage (b).[35] The AFM image of a virus containing film (c), and its fluorescence (d).[9]

Electrically conductive thin films are especially interesting for applications such as EMI shielding, electrostatic dissipation, touch screen electrodes, and flexible sensors. Many of these applications require transparency.[36] The thin nature of LbL films has even resulted in transparent films with carbon black,[21] but combining high transparency and conductivity requires the use of intrinsically conductive polymers (ICP). In this research, thin films have been deposited using water-dispersed colloids of poly(3,4-ethylenedioxythiophene) (PEDOT) doped with poly(styrene sulfonate) (PSS). Figure 4 shows a schematic of the PEDOT-PSS chemistry. PEDOT itself is not water soluble so water soluble PSS is added as a dopant. The resulting particles have a net negative charge due to the strong anionic nature of PSS, which provides the basis for layer-by-layer assembly with a polycation. Many studies of the electrochromic behavior of PEDOT based assemblies have already been performed,[37-39] but little work has been done to tailor the electrical conductivity of these films or protect them from UV degradation.

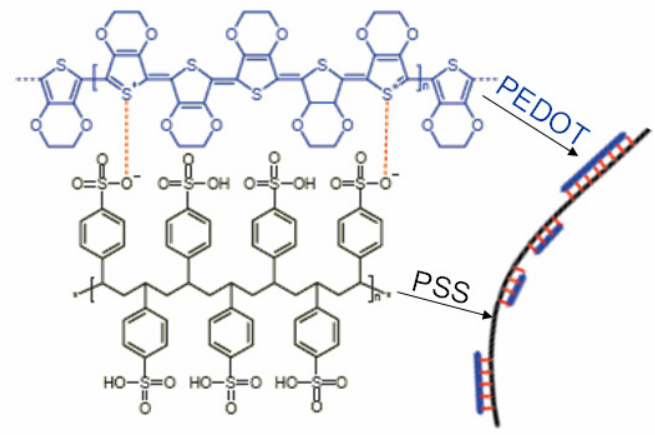

Figure 4. Schematic showing PEDOT-PSS chemistry.[40]

Intrinsically conductive polymers have conjugated backbones (i.e. alternating single and double bonds) and the electrical charge passes along the π orbitals on the polymer backbone.[41] In 1977, H. Shirakawa, Alan G. MacDiarmid, and A.J. Heeger, found that polyacetylene films doped with arsenic pentafluoride were significantly more conductive than undoped films.[42] This work led to a Nobel Prize in Chemistry in 2000. Significant changes in sheet resistance can be achieved by doping, which can be achieved by a redox reaction (reduction or oxidation). PEDOT-PSS is effectively doped with dimethyl sulfoxide (DMSO) which oxidizes and partially dissolves the particle.[43] Solvation causes PEDOT particles to swell and intermesh with other particles and better align its chains, thus increasing the electrical conductivity. Particle size is also tightly tied to conductivity, as particle size decreases so does the conductivity.[40] This is due to the difficulty of the charge transferring from one particle to another (the larger the particles, the fewer the transfers).

PEDOT-PSS has been used in a variety of applications including electrochromic,[13,44] light emitting diodes,[45,46] and transistors.[47] PEDOT films have been made via spin coating,[48] sputter coating,[49] and LbL assembly.[37] In spin coating, the polymer solution (or suspension) is deposited onto a spinning substrate. The thickness of the film depends on the angular speed and polymer concentration,[50] with higher speed producing thinner films. The drawback to spin coating is that the film is not completely uniform and does not follow the topology of the substrate very well. In sputter coating, a solid material is deposited onto a substrate in a

vacuum by colliding the depositing material with ions.[51] Atoms are ejected away from the solid and coat the surface of the substrate. Lack of ambient conditions for deposition is the biggest drawback of sputter coating.

PEDOT-PSS films made via the LbL assembly technique are described in the following chapters. Processing and compositional variables were evaluated in relation to electrical conductivity and UV-susceptibility of the thin films. Chapter II focuses on film growth and conductivity in the absence of UV protection. Cationic polymer choice and effect of doping are evaluated with respect to film thickness, conductivity and transparency. Chapter III examines the increase in resistance due to UV aging and the addition of nanoparticles to prevent this effect. Like most ICPs, PEDOT is inherently susceptible to environmental degradation.[52] UV absorbing particles like titanium dioxide can absorb UV light,[33] thus providing protection for PEDOT. Titanium dioxide (TiO_2) is used extensively in polymers to increase the UV resistance,[53] whereas carbon black is used as a pigment[54] or an electrically conductive filler.[21] The ability of these UV-absorbing particles to reduce UV degradation was evaluated. Chapter IV discusses applications for these conductive films and some thoughts on future LbL work with magnetic particles and quantum dots.

CHAPTER II

FILM GROWTH AND ELECTRICAL CONDUCTIVITY

Introduction

Layer-by-layer deposition of PEDOT-PSS with a suitable polycation allows for tunable sheet resistance and optical transparency. The goal is to reduce sheet resistance while minimizing film thickness and increasing optical transparency. In general, the more conductive a sample the thicker or less transparent it is.[21] By carefully manipulating specific processing variables these film properties can be finely tailored. The variables studied here include doping of PEDOT-PSS, varying polycation pH and concentration and changing the type of polycation.

Experimental

Materials. Cationic deposition solutions were prepared with 0.1 or 0.3 wt% of either branched polyethylenimine (BPEI) (with a molecular weight (MW) of 25,000 g/mol), linear polyethylenimine (LPEI), with MW of 25,000 g/mol, or poly(allylamine hydrochloride) (PAH) (with MW of 70,000g/mol). Polymers were purchased from Aldrich (Milwaukee, WI). The anionic deposition mixture contained 0.3 wt% PEDOT-PSS (tradename BAYTRON P HC V4) that was purchased from H.C. Starck (Newton, MA). The P HC V4 had a PEDOT to PSS ratio of 1:2.5 by weight.[55] Where indicated, 1M HCl was used to reduce the pH of PEI solutions. Poly(ethylene terephthalate) (PET) film (tradename ST505 by DuPont Teijin) (Tekra Corp., New Berlin, WI), (1 0 0) silicon wafers polished on

only one side (University Wafer, South Boston, MA), standard glass microscope slides (VWR, West Chester, PA) and fused quartz glass slides (Structure Probe Inc., West Chester, PA) were used as substrates for deposition. This wide variety was necessary to accommodate the various characterization techniques used (see below). Dimethyl sulfoxide (DMSO), purchased from Aldrich, was used as a dopant for PEDOT-PSS at a concentration of 1 wt% of the mixture weight.

Film Deposition. All films were deposited following the procedure shown in Figure 5. The initial dip into each mixture was 5 minutes, beginning with the cationic solution. Subsequent dips were 1 minute. Following deposition of all layers, the films were oven dried at 70^0C for 15 minutes. For deposition onto PET, the samples were cut to size, rinsed with methanol then de-ionized water and dried with filtered air. The cleaned PET substrates were then corona treated with a BD-20C Corona Treater (Electro-Technic Products Inc., Chicago, IL). Corona treatment oxidizes the surface of PET which allows the polycationic polycation to better adhere.[56,57] For deposition on fused quartz slides piranha treatment was performed.[58] The slides were removed from piranha solution after sonicating for 30 minutes, thoroughly rinsed with de-ionized water and dried with filtered air. The silicon wafer and glass microscope slides were rinsed with acetone then de-ionized water and finally dried with filtered air, with no additional surface treatment performed. Films made with more than 14 BL were prepared with a home-built robotic dipping

system.[59] All films were stored in a dry box for a minimum of 12 hours before testing.

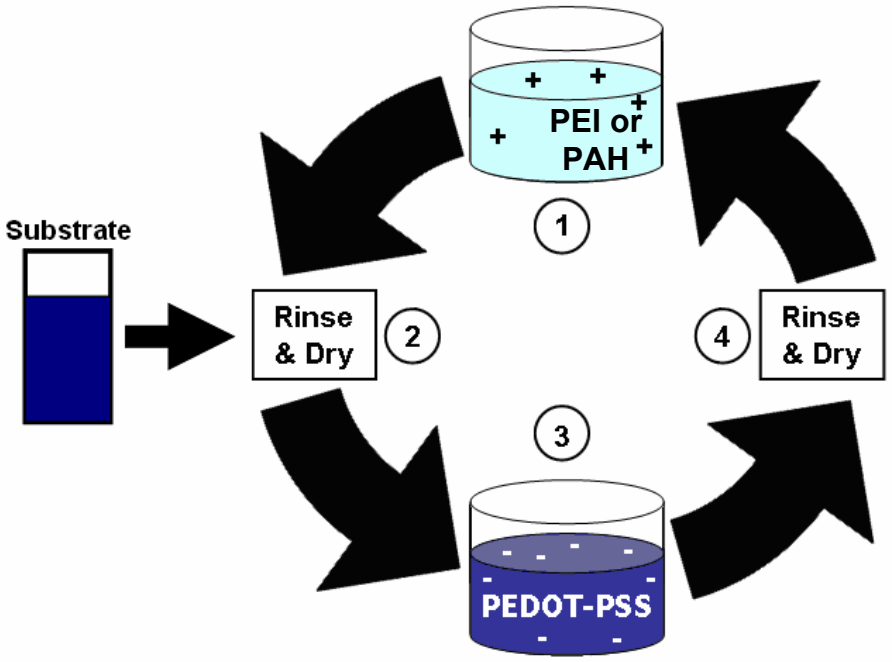

Figure 5. Schematic of the LbL deposition process, each revolution will deposit one bilayer. Note the polycation was either polyethylenimine (PEI) or poly(allylamine hydrochloride) (PAH).

Characterization. Film growth was monitored with a USB2000-UV-VIS Spectrometer (Ocean Optics, Dunedin, FL). The absorbance was measured between 190 and 900nm. Thickness was directly measured with a Dektak 3 Profilometer (Veeco Instruments, Woodbury, NY), a Research Quartz Crystal Microbalance (Maxtek Inc., Cypress, CA), or from a PHE-101 Discrete Wavelength Ellipsometer with a wavelength of 632.8nm and an angle of 65° (Microphonics, Allentown, PA). Sheet resistance was measured with a home-built four point probe apparatus. A 2000 Multimeter (Keithley, Cleveland, OH) with a Signatone probe head (Lucas Labs, Gilroy, CA) and an E3644A power supply (Agilent Technologies Inc., Santa

Clara, CA) were used in conjunction with LabView 6 (National Instruments, Austin, TX) for data processing. Thin film cross sections were imaged with a JEOL 1200EX TEM (Peabody, MA) and surface images were from a Vega II SEM (Tescan, Czech Republic). All SEM samples were sputtered with 4nm of platinum.

Results and Discussion

Figure 6 shows how doping dramatically reduces the sheet resistance in films made with 0.3 wt% BPEI and 0.3 wt% PEDOT-PSS mixtures. As discussed below, these films are less than 1 μm thick (with the exception of 12BL films) and can have a bulk resistivity of 0.3 Ω-cm.[55] Pure PEDOT has a bulk resistivity of approximately 0.005 Ω-cm. The elevated resistance in these LbL films is due to the insulating cationic polymer (polyethylenimine in this case) used in the assembly process. By doping the PEDOT-PSS solution with 1wt% DMSO the sheet resistance can be decreased by approximately 85%. For example, an undoped 8-bilayer film has a sheet resistance of 84,700 Ω/sq that is reduced to 14,300 Ω/sq when doped with DMSO during deposition. DMSO is known to solvate the PEDOT, which leads to chain alignment and lower resistance. [60]

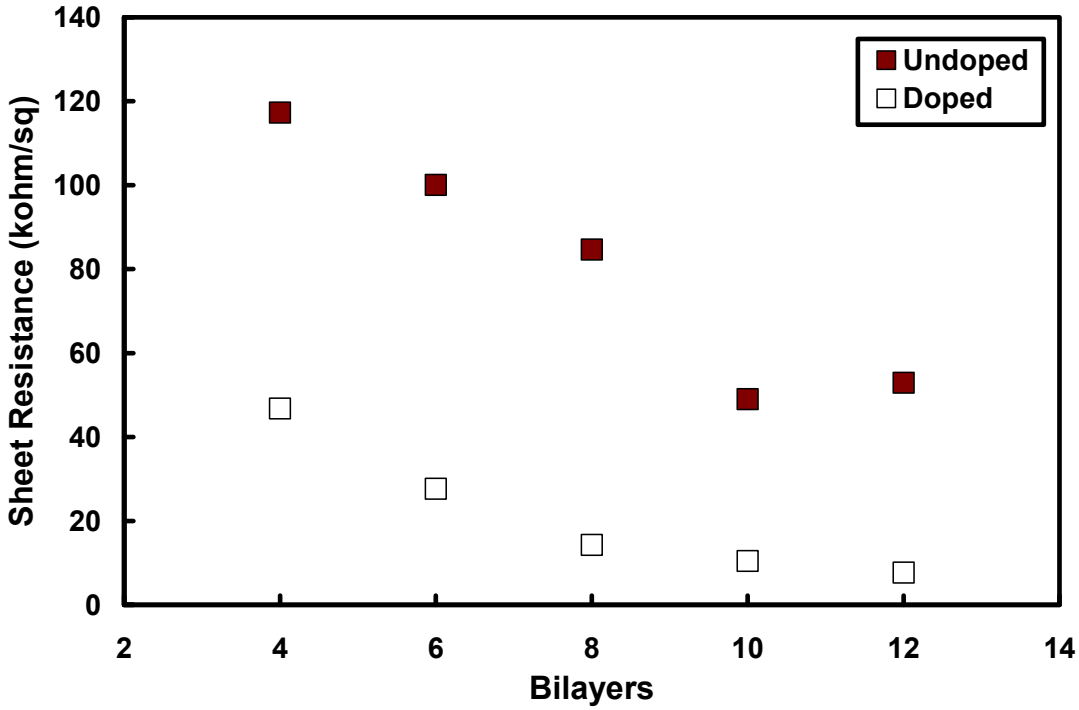

Figure 6. Sheet resistance as a function of bilayers deposited for thin films made with 0.3wt% BPEI + 0.3wt% PEDOT-PSS. The PEDOT-PSS solution was doped with 1wt% DMSO where indicated.

These films show what appears to be exponential increase in growth for each additional bilayer deposited. This is due in part to the diffusion of the polyelectrolytes into the deposited film in addition to a growing charge imbalance as the film grows. Absorbance measurements show that both the doped and undoped PEDOT-PSS films grow at the same rate. By taking the absorbance at 550 nm the film growth can be monitored as seen in Figure 7. This growth closely resembles that observed by others studying PEDOT-based assemblies,[61-63] who suggest film growth is composed of two linear regimes rather than exponential.

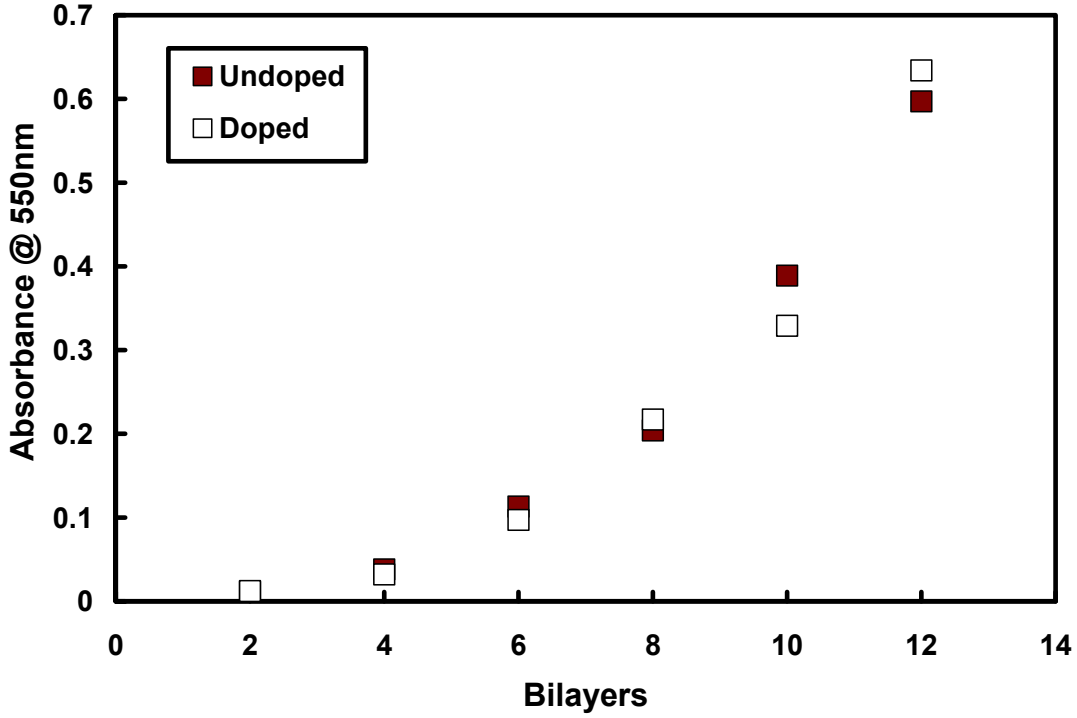

Figure 7. Absorbance at 550 nm as a function of bilayers deposited for films made with 0.3wt% BPEI + 0.3wt% PEDOT-PSS. The PEDOT-PSS solution was doped with 1wt% DMSO where indicated.

Absorbance measurements can be converted into transmission, using Beer's Law (A=abc). Figure 8 shows how each bilayer deposited reduces visible light transmission. Since both the doped and undoped films are growing at the same rate their percent transmission values are very similar. At 12 bilayers the films are only 50% transparent. Figure 8 also shows the thickness of each film as measured with ellipsometry. Ellipsometric thickness better shows the two linear growth regimes suggested by others.[62] The first linear regime can be attributed to packing density

alteration due to substrate influence. This data also confirms that doping has little influence on film thickness.

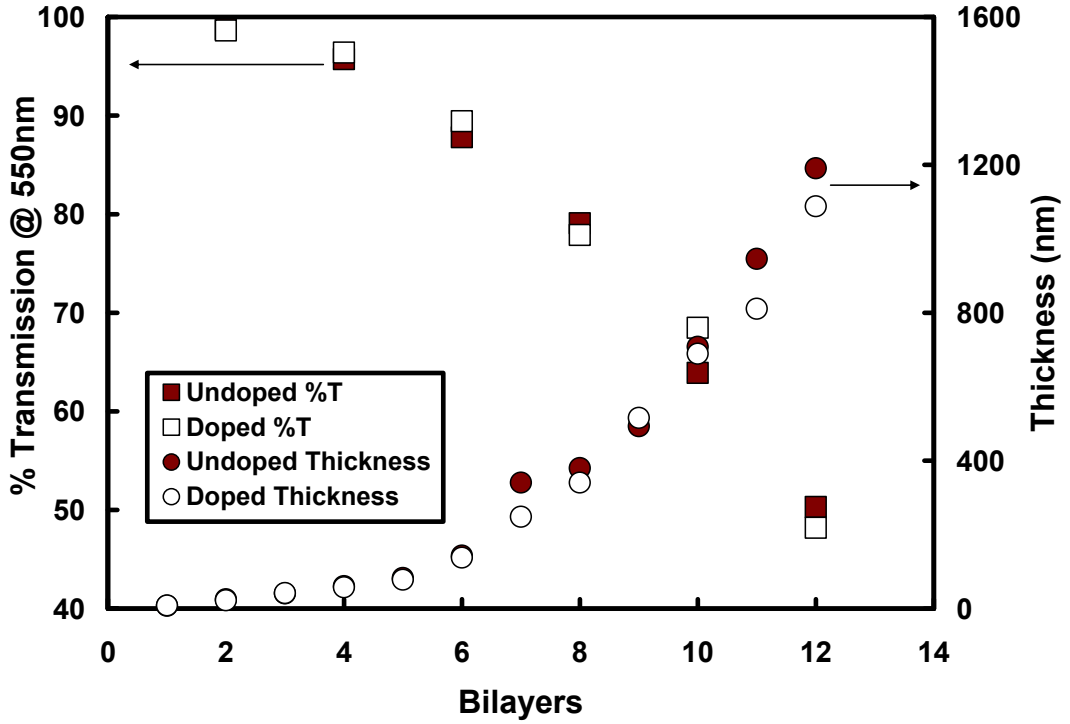

Figure 8. Percent transmission at 550nm and thickness as a function of bilayers deposited for films made with 0.3wt% BPEI + 0.3wt% PEDOT-PSS. The PEDOT-PSS solution was doped with 1wt% DMSO where indicated.

As already mentioned, DMSO increases the conductivity of these films by partially dissolving the PEDOT-PSS particles. This solvation swells the colloidal PEDOT-PSS particles. Figure 9 shows AFM surface images that show this effect. The doped PEDOT-PSS particles (Fig. 9(b)) are larger than the undoped form. (Fig. 9(a)). The boundaries between particles also appear to be softened in the doped film, which contributes to lower resistance.

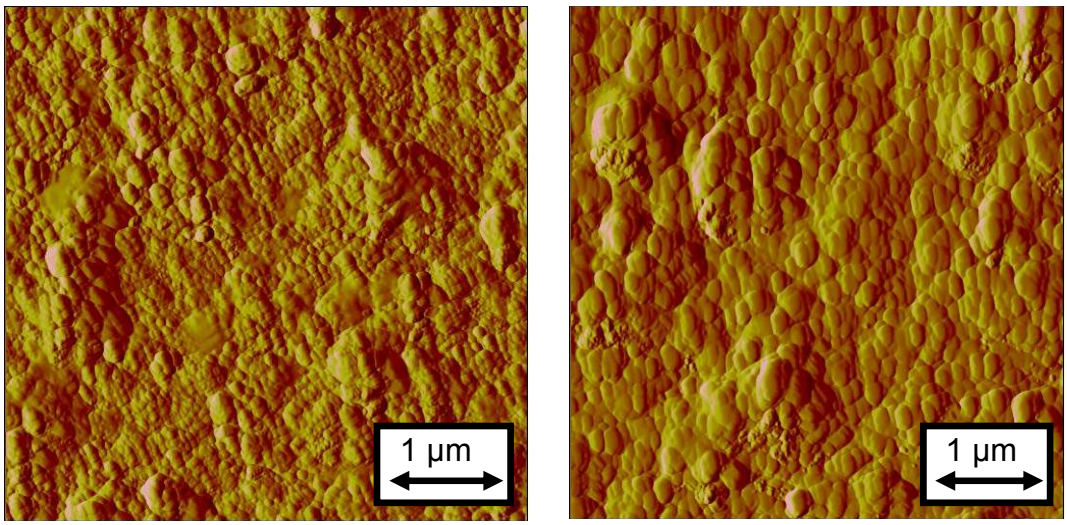

Figure 9. AFM phase images of undoped (a) and doped (b) 12BL films. These films were produced by alternately depositing BPEI and PEDOT-PSS. In doped films, the PEDOT-PSS mixture contained 1wt% DMSO.

Figure 10 shows the effect of doping concentration. If the concentration of DMSO is varied the PEDOT-PSS particles will dissolve and swell to different extents. The optimum amount of dopant was found to be 1wt%. Other doping levels (0.2 and 5 wt%) were evaluated, but their sheet resistance was closer to the undoped films until 12 bilayers. It is believed that too little DMSO yields poor chain alignment, while too much may result in weaker contacts between chains.

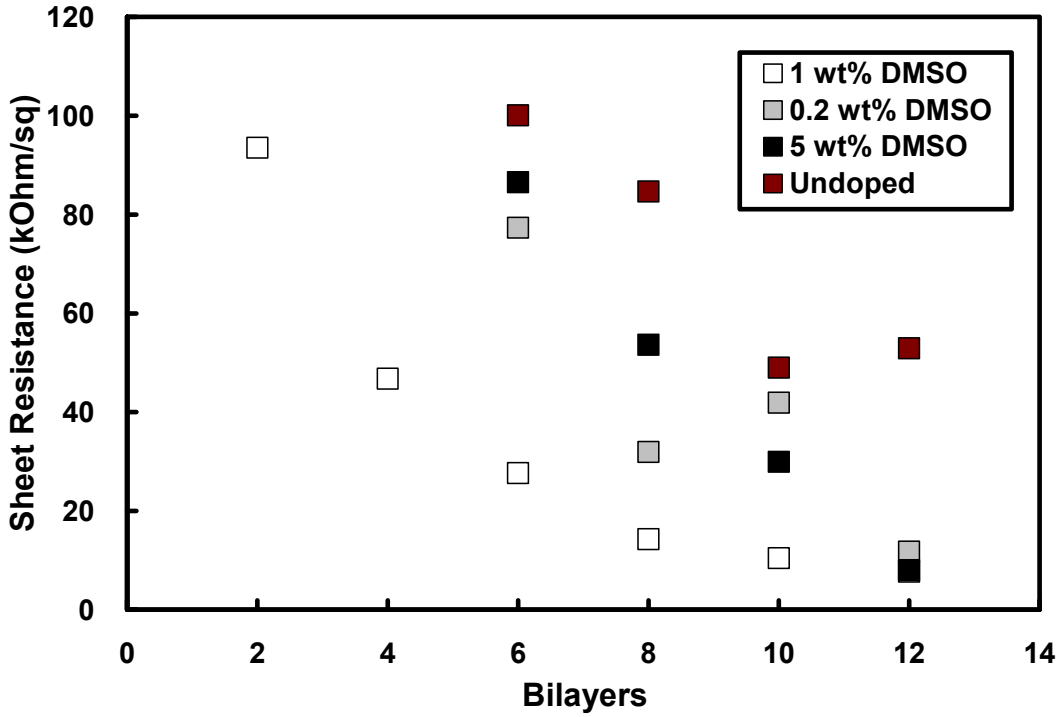

Figure 10. Sheet resistance as a function of bilayers deposited for films made with 0.3wt% BPEI + 0.3wt% PEDOT-PSS. The PEDOT-PSS solution was doped with 0.2, 1, and 5wt% DMSO where indicated.

PEI is an electrically insulating polymer, which is layered between conductive PEDOT colloids and acts to reduce the electrical conductivity of these LbL films. As a result, film conductivity can be increased by decreasing the concentration of PEI in the deposition solution. Figure 11 shows that the sheet resistance of a 4 BL film decreases ~60% by using 1 wt% BPEI along with doping the PEDOT with 1 wt% DMSO. 12BL films with 0.1 wt% BPEI with un-doped PEDOT actually has the same sheet resistance as doped 0.3 wt% BPEI, suggesting that decreasing the weight percent is as effective as doping for electrical conductivity of LbL assemblies.

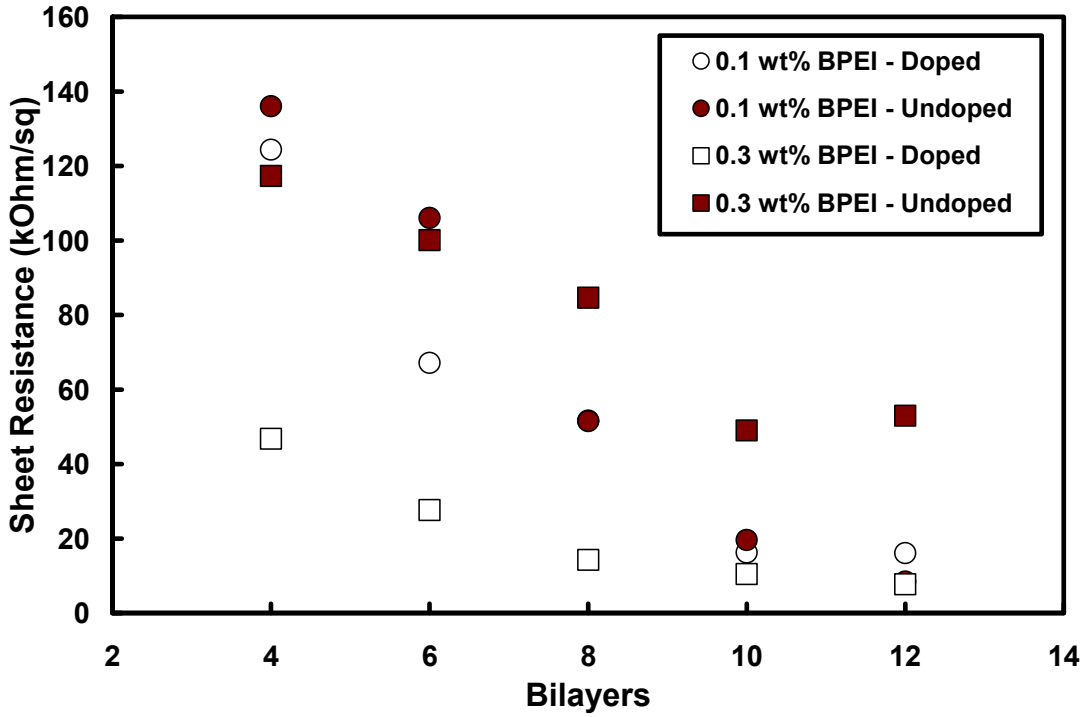

Figure 11. Sheet resistance as a function of bilayers deposited. The PEDOT-PSS mixture was 0.3wt% in all cases and the PEDOT-PSS mixture was doped with 1wt% DMSO where indicated.

If the thickness for each deposited PEI layer is reduced, the absorbance and total film thickness should also be reduced for each bilayer. Figure 12 shows that the absorbance at 550nm for the 0.1 wt% films is indeed lower than the 0.3 wt% films. It also shows that the doped form of PEDOT actually has a lower absorbance than the undoped, but ellipsometry data for the undoped forms of both the 0.3 and 0.1 wt% PEI films are very similar. The ellipsometry and absorbance readings show very similar growth until about the 6th bilayer. After that point the 0.3 wt% PEI films grow at a greater rate in absorbance, while the thickness growth (measured via ellipsometry) is similar until about the 11th bilayer. This is likely due to doped PEDOT having swollen PEDOT-PSS particles that increase the thickness without increasing the absorbance.

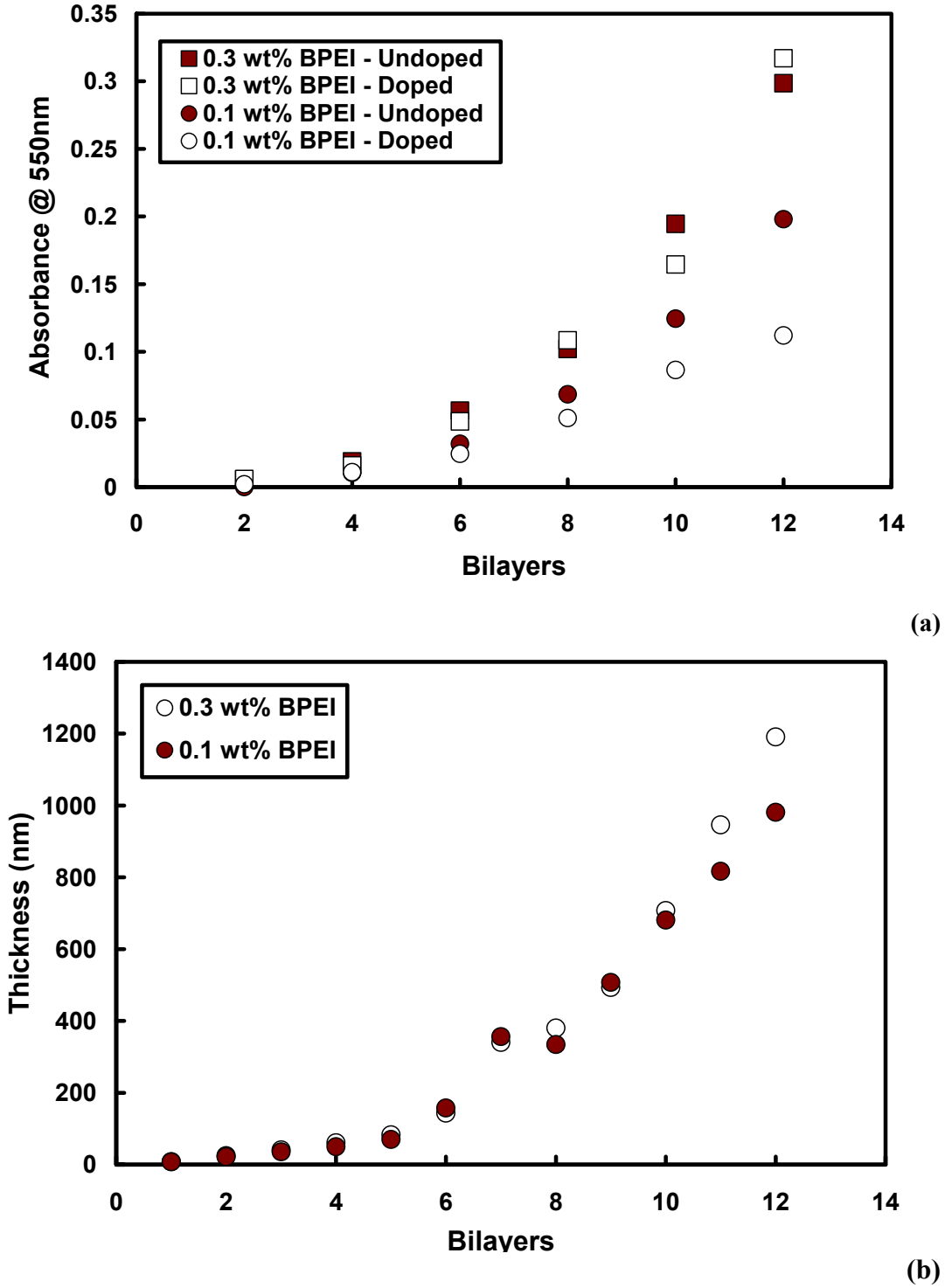

Figure 12. Absorbance at 550nm (a) and ellipsometric thickness (b) as a function of bilayers deposited. The PEDOT-PSS mixture was doped with 1wt% DMSO where indicated.

Another method used to decrease the PEI layer thickness is to use linear PEI (LPEI). This linear structure will allow the sample to deposit thinner than the branched form used up to this point. Branching along the polymer backbone will not allow the polyelectrolyte to lie as flat on the surface. By utilizing LPEI, the deposited thickness for each layer will decrease. This minimizes the barrier between PEDOT particles, as was done by decreasing the concentration of BPEI. Figure 13 shows sheet resistance as a function of bilayers deposited for BPEI and LPEI. Unlike BPEI, altering the LPEI weight percent has very little effect on the sheet resistance for the films.

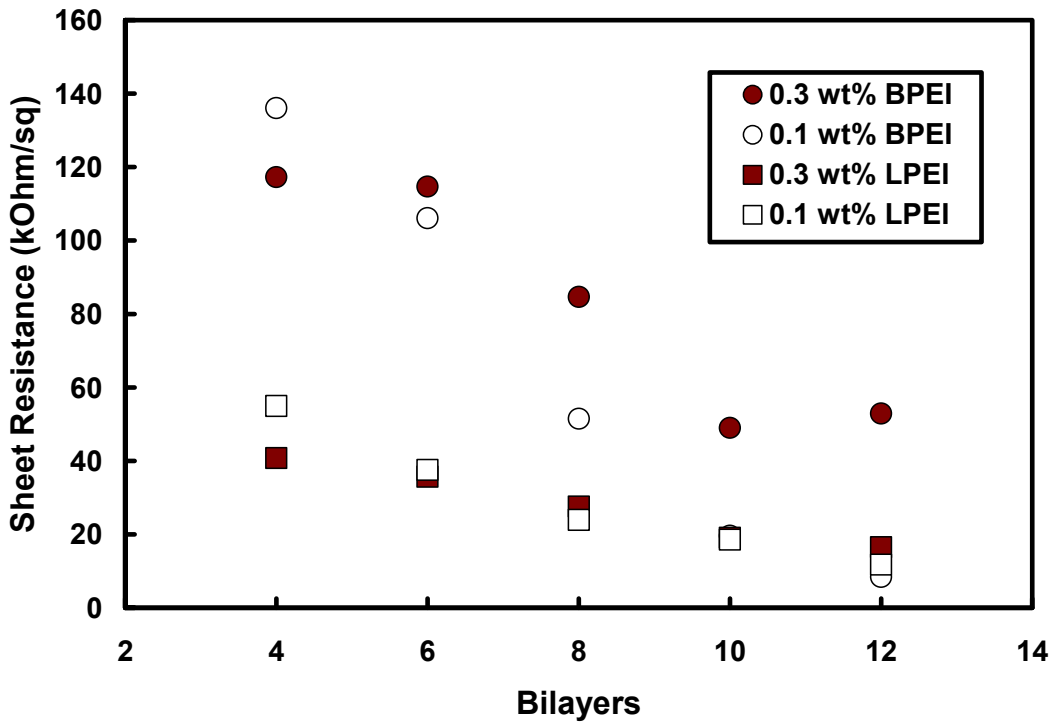

Figure 13. Sheet resistance as a function of bilayers deposited for films made with 0.3wt% PEDOT-PSS with 0.1 or 0.3wt% BPEI or LPEI.

Figure 14(a) confirms that altering the LPEI concentration has very little effect on thickness, much like sheet resistance (Fig. 13). At 11 BL, the 0.3 wt% LPEI film is approximately 900nm, while the BPEI is near 1 μm. Before the fourth bilayer the film growth is spotty for LPEI-based films, but growth is very linear once the surface is sufficiently covered. The absorbance for both the 0.1 and 0.3wt% solutions are also linear (Fig. 14(b)). Values for 0.1wt% LPEI are less than half that of 0.3wt%, while the thickness remains similar for both. This is a reasonable result if the density of the 0.1wt% films is less than half the 0.3wt% film, which is possible for thin films.

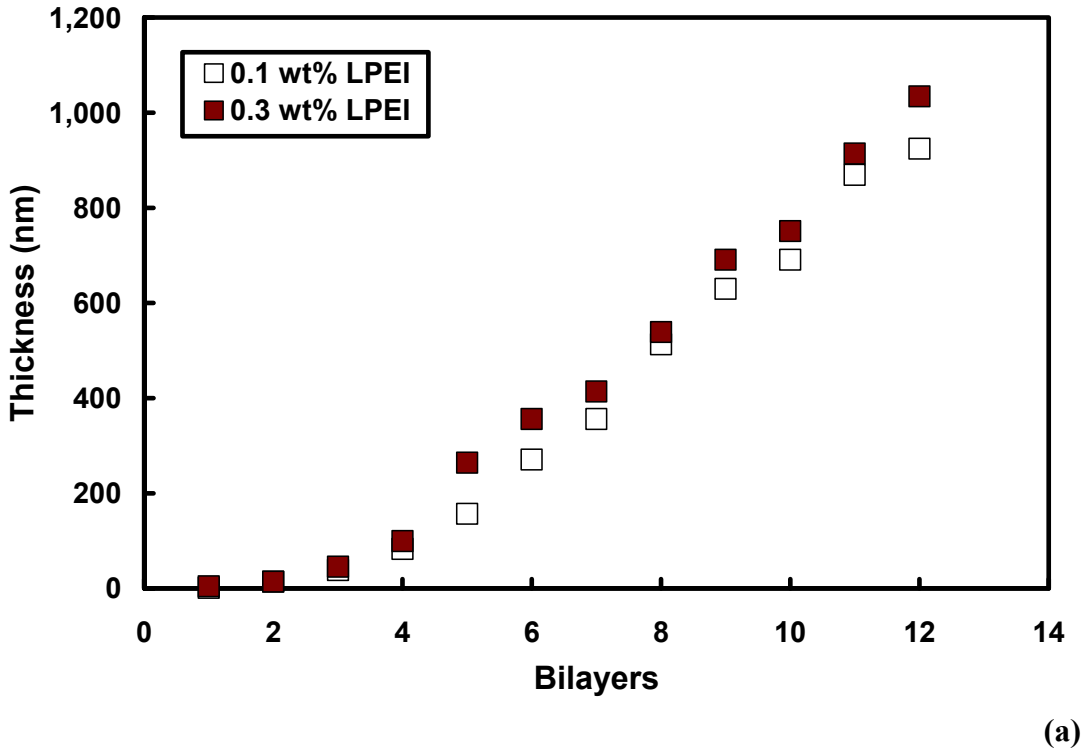

Figure 14. Ellipsometric thickness (a) and absorbance at 550nm as a function of bilayers deposited. In all cases films were made with 0.3wt% PEDOT-PSS.

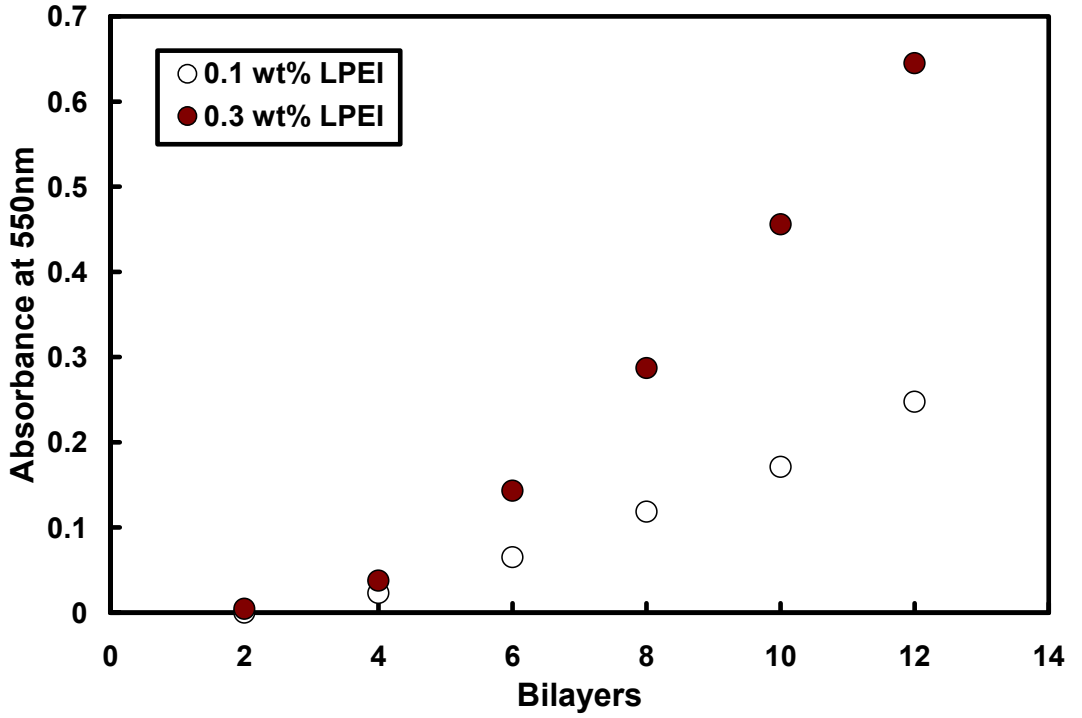

(b)

Figure 14. (continued)

The addition of salt to the PEI solution has been shown to adversely alter the conductivity, as shown in Figure 15, by restricting the growth of the conjugated bond length.[64] The most conductive recipe, 0.1wt % LPEI alternated with 0.3 wt % PEDOT-PSS, had 1, 10, and 100 mM concentrations of NaCl added to the cationic LPEI . The resistance of the initial bilayers with salt was too high to accurately measure with the four-point probe. Resistance values get closer to one another at higher bilayers, which is likely due to salt ions being rinsed out of the films.

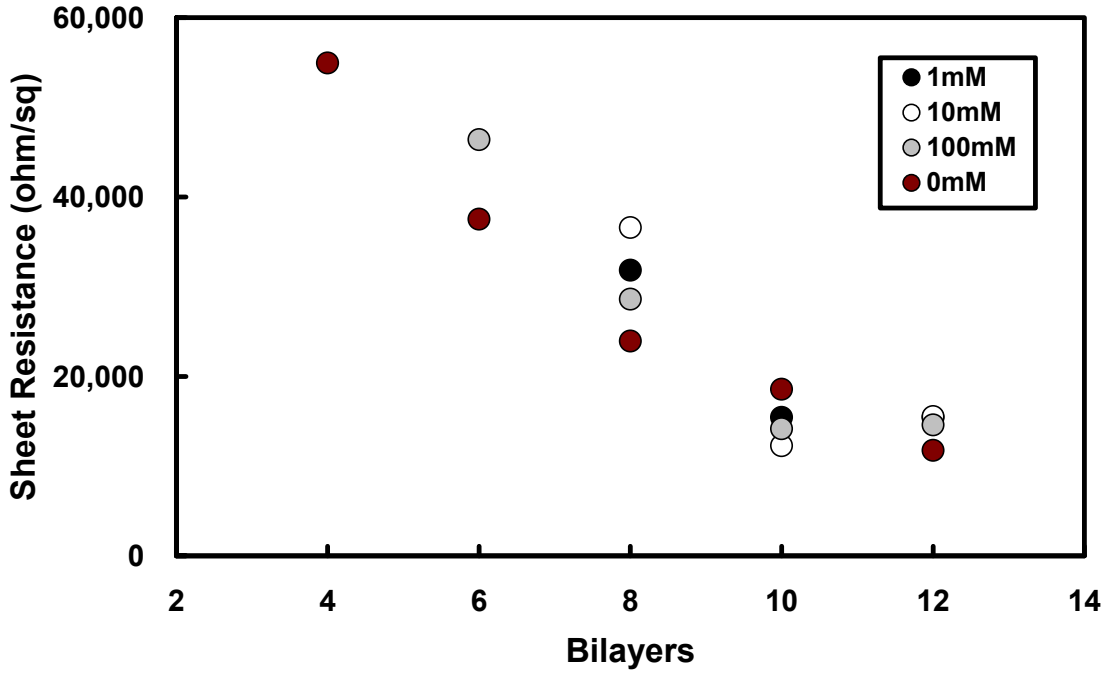

Figure 15. Sheet resistance as a function of bilayers deposited for films with varying concentrations of NaCl added to 0.1 wt% LPEI alternated with 0.3 wt% PEDOT-PSS.

Increasing the charge density of the polycation is an additional way to reduce thickness, as higher charge density polymers lie flatter on the substrate.[22,25,30] This can be accomplished by changing the polycation type or simply reducing the pH of the PEI solution. Decreasing the pH of the PEI solution increases the cationic charge on the polymer's backbone, which in turn allows the deposition thickness be reduced.[22] Within the range of a half unit of pH the deposition layer thickness can increase significantly, as shown in Figure 16. The pH = 10.2 system is the natural pH of 0.3wt% BPEI, while the other samples had their pH reduced with 1 M HCl.

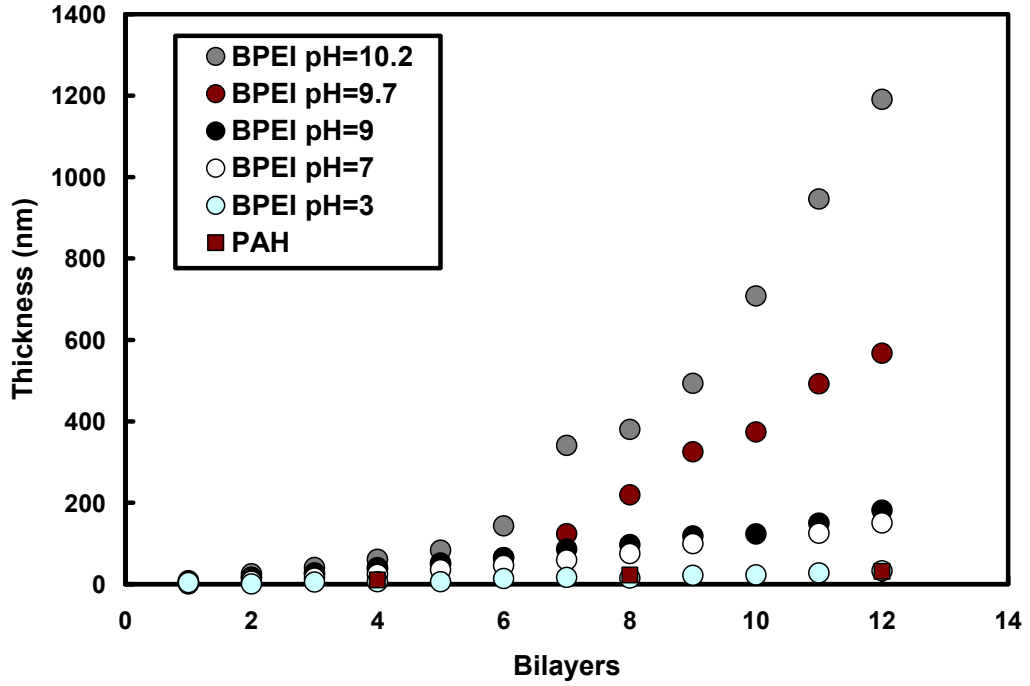

(a)

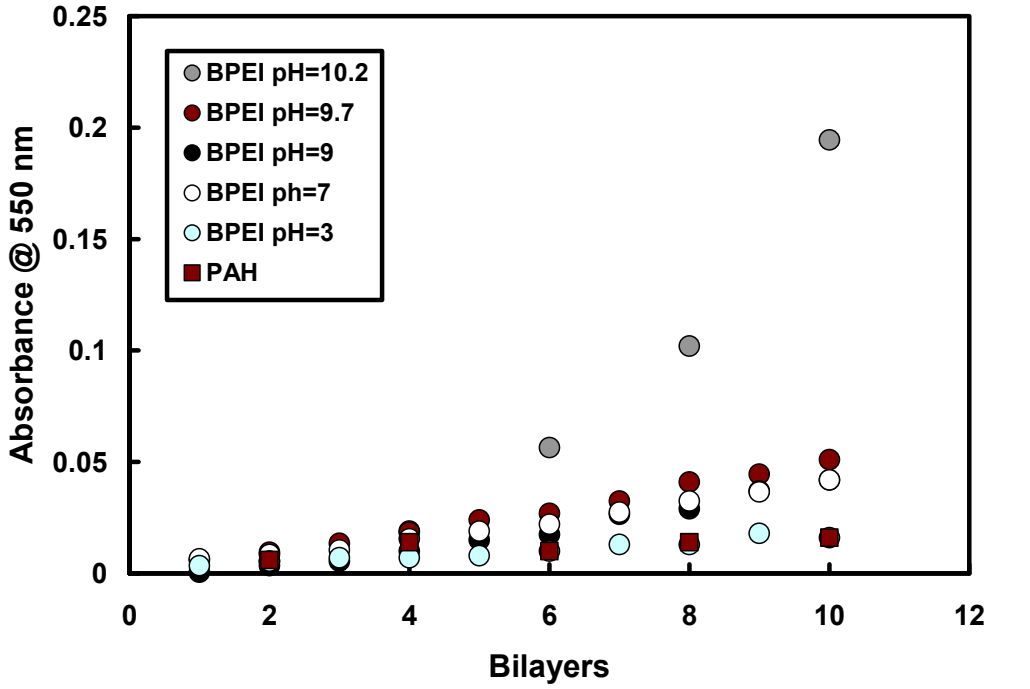

(b)

Figure 16. Ellipsometric thickness (a) and absorbance at 550nm (b) as a function of bilayers deposited. In all cases films were made with 0.3wt% PEDOT-PSS and 0.3wt% BPEI. The pH was adjusted with 1M HCl.

Figure 17 shows how thin and linear the deposition of PAH is up to 40 bilayers, which agrees with the findings of others.[65] Each bilayer is approximately 2 nm and is far thinner than the PEI system that was approximately 100 nm after only 5 bilayers. However, the sheet resistance of the PAH system was too high to accurately measure, even at 40 bilayers. Similar results were found when the pH of BPEI was reduced from ~10 down to 3, which is known to make each imine group fully charged.[66]

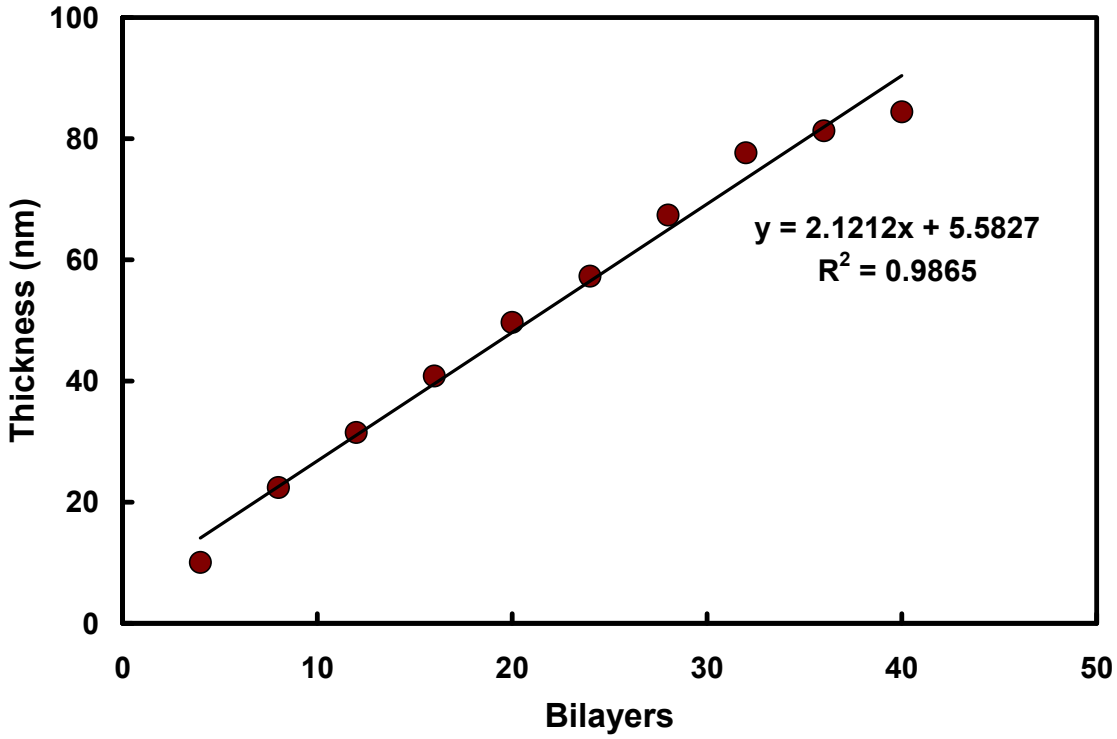

Figure 17. Thickness of 0.3 wt% PAH and 0.3 wt% PEDOT-PSS, as a function of bilayers deposited, measured via ellipsometry.

Whereas doping increased the conductivity with the PEI/PEDOT-PSS system there was little measurable increase in the conductivity of the PAH system. The resistance was still too high to accurately measure. Using an AFM, the surface was

imaged and the doped PEDOT particle size was larger than the undoped form, as shown in Figure 18.

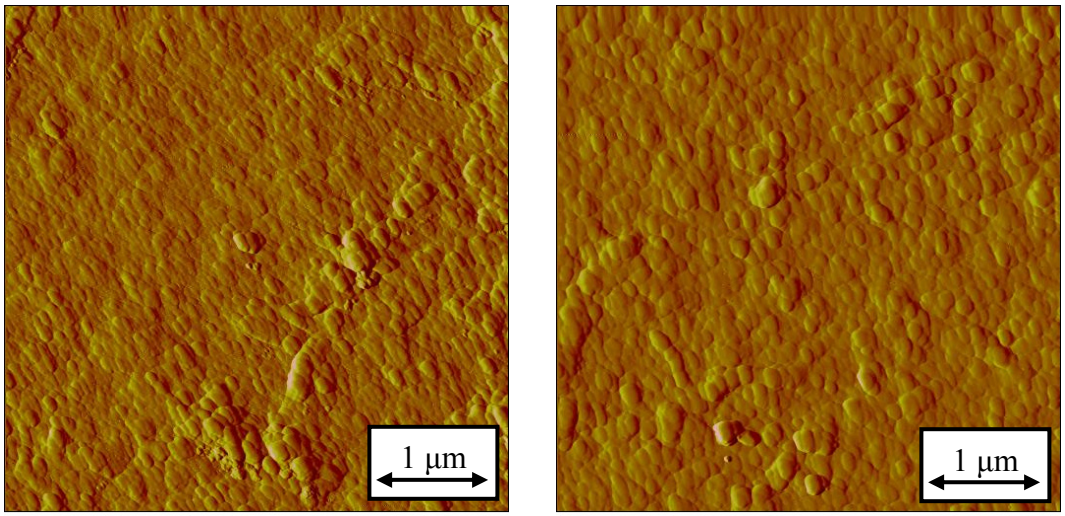

Figure 18. An AFM phase image of the surface of undoped (a) and doped (b) 12BL films. These films were produced by alternately depositing PAH and PEDOT-PSS. In doped films, the PEDOT-PSS mixture contained 1wt% DMSO.

Conclusion

Doping and choice of polycation have a significant influence on bulk resistivity and film growth for layer-by-layer assemblies of PEDOT-PSS. These films can have a bulk resistivity below 1 Ω-cm, thickness below 100 nm and transparency greater than 90%. This makes these films suitable for applications such as low conductivity electrodes used in flexible displays. Films made with PEI had a growth rate more than an order of magnitude larger than PAH films and were up to 3 times more conductive when doped. Doping with 1 wt% DMSO provided the maximum improvement in conductivity for doped films. Further work will focus on improving electrical conductivity with different dopants, polyelectrolytes and fillers.

CHAPTER III

UV DEGRADATION OF ELECTRICAL CONDUCTIVITY

Introduction

Chapter II focused on tailoring the electrical conductivity of the PEDOT-PSS films, while Chapter III deals with the ultraviolet degradation of electrical conductivity. Intrinsically conductive polymer conductivity degrades by two methods when exposed to light, scission of the backbone and the creation of defects.[52,67,68] UV absorbing particles such as TiO_2 and carbon black (CB) can be added to help prevent this degradation. In the present work, nanoparticles of TiO_2 and CB were added to LbL films to enhance the stability of the PEDOT. Initial bilayers were deposited as shown in Chapter II, but after the initial bilayers were deposited, the cationic solution was exchanged with a cationic solution containing 0.05 wt% BPEI and 0.25 wt% of either TiO_2 or CB. As Figure 19 illustrates, there are UV absorbing particles in the top layers of the film as a result.

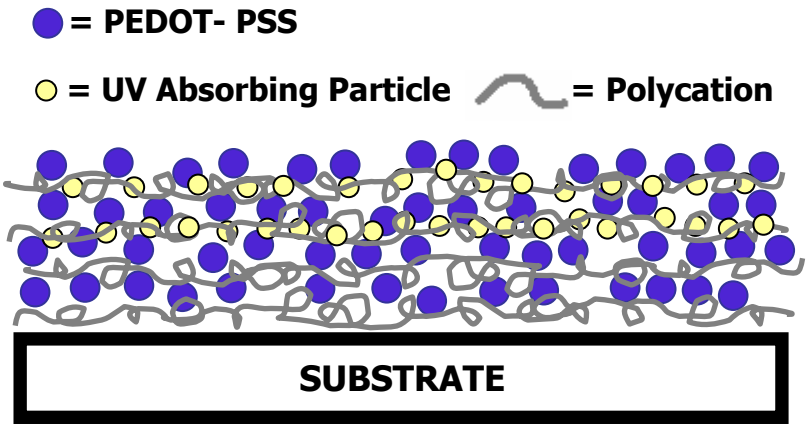

Figure 19. Schematic of a multilayer film with UV absorbing particles in the outer layers.

Experimental

Materials. Conductex 7055 Ultra was the carbon black used here (Columbian Chemicals, Marietta, GA), which has a 42 nm particle size. The colloidal TiO_2 (tradename Pinnacle Titanium Dioxide) was provided by Applied NanoWorks (Rensselaer, NY) and has a 10nm particle size. When CB or TiO_2 were added, to the BPEI solutions, 0.05 wt% polymer was used with 0.25 wt% CB or TiO_2, otherwise the solution contained just 0.3 wt% polymer. The same substrates described in Chapter II were also used here.

Film Deposition. Initial bilayers contained no UV absorbing particles. For films designated "6-6", the first 6 bilayers were the standard recipe (0.3wt% BPEI and 0.3wt% PEDOT-PSS), while the next 6 used the cationic solution containing the UV absorbing particles. In the case of the 3-1 TiO_2 film, the first 3 bilayers were the standard recipe followed by one UV absorbing bilayer. This was repeated 3 times to create a 12 BL film. In other words, 12 BL films were used for all UV degradation studies.

Characterization. These films were exposed to 365 nm light from a Black-Ray UV Bench Lamp (UVP, Upland, CA) and further characterized with the techniques described in Chapter II.

Results and Discussion

The initial sheet resistance of each film, prior to UV-light exposure, was measured and recorded in Table 1. The samples were then exposed to 365nm light at an intensity of 2.16 W/cm^2. The total time the samples spent under the UV lamp was 781,250 seconds (~9 days). After only 20 minutes (1250 s) the sheet resistance had increased noticeably. The samples all began with a sheet resistance of 30,000 ± 3,000 Ω/□, but these values were divided by the initial resistance reading to normalize the data. Figure 20 shows the increase in sheet resistance as the exposure time is increased. Note how the pure sample is 4 times less conductive (more resistive) than the sample with 6 BL of TiO_2 protection and 5 times less conductive than the sample with TiO_2 in every bilayer. Carbon black is a conductive filler, but did not improve the conductivity of the film. Furthermore, TiO_2 is a much more effective protectant than CB. This was somewhat surprising due to the highly absorbing nature of CB across the UV-vis spectrum.

Table 1. Sheet resistance values for PEDOT-based assemblies exposed to UV light.*

Time (s)	Pure (Ω/□)	6-6 TiO2 (Ω/□)	9-3 TiO2 (Ω/□)	6-6 CB (Ω/□)	9-3 CB (Ω/□)	3-1 TiO2 (Ω/□)	All TiO2 (Ω/□)
1	30,876	29,715	27,012	35,444	32,202	23,548	40,457
10	29,963	31,414	24,932	30,152	26,767	27,296	38,382
50	31,964	33,232	26,124	30,465	26,687	28,425	38,575
250	38,042	40,296	32,813	33,279	26,720	34,134	40,455
1,250	52,736	49,594	47,602	45,177	36,481	43,474	51,950
6,250	50,379	48,687	38,603	44,344	37,606	38,327	48,462
31,250	98,891	79,980	64,391	80,025	73,525	72,709	80,001
156,250	313,109	164,609	142,670	173,083	186,005	187,220	127,215
781,250	1,655,549	404,642	435,717	692,651	776,059	905,744	325,539

* The first number denotes the number of bilayers without UV absorbing particles. All films were 12 BL total. The 3-1 film had one UV absorbing bilayer for every 3 standard bilayers.

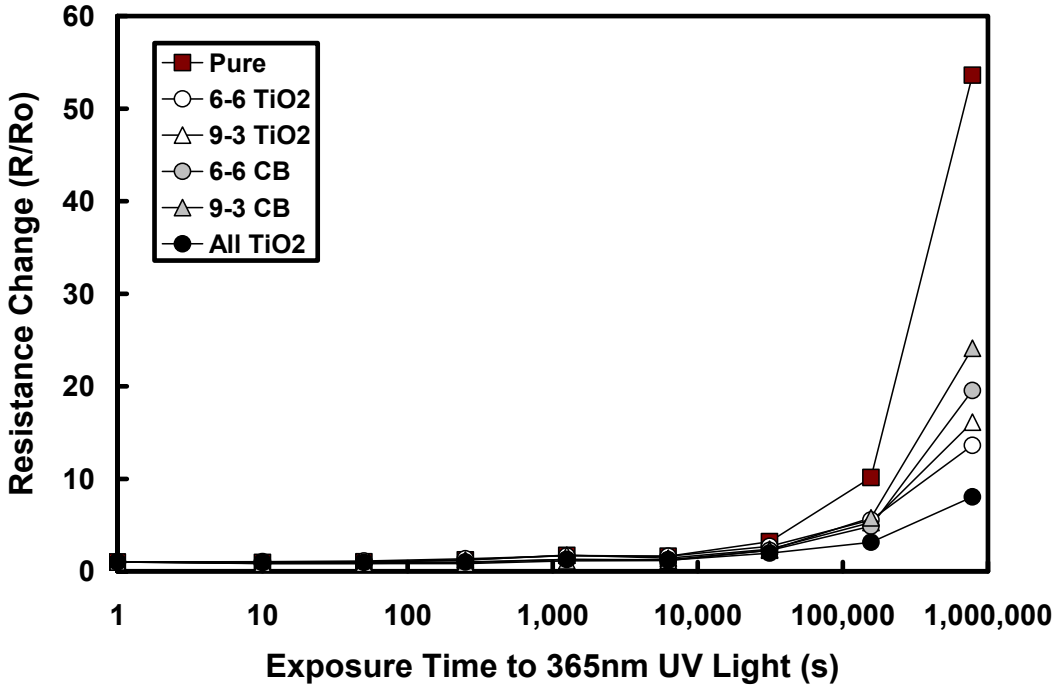

Figure 20. Normalized change in sheet resistance as a function of time exposed to the UV light. All films began with a sheet resistance near 30,000 Ω/□ (+/- 10%).

In addition to being more electrically conductive following UV exposure, the film with TiO_2 in all bilayers was also the most transparent. Figure 21 shows the transparency measurements. The samples with carbon black were the least transparent. The TiO_2 was stabilized with acetic acid and when mixed with the 0.05 wt% BPEI the pH was lowered to approximately 4. This pH reduction made the BPEI deposit much thinner (due to greater charge density) than the unmodified, high pH BPEI. Transparency and conductivity are also linked to the discrete nature of the 8 nm TiO_2 colloids in the assemblies. Carbon black is much more aggregated, which increases opacity and serves to prevent PEDOT layers from interacting as strongly.

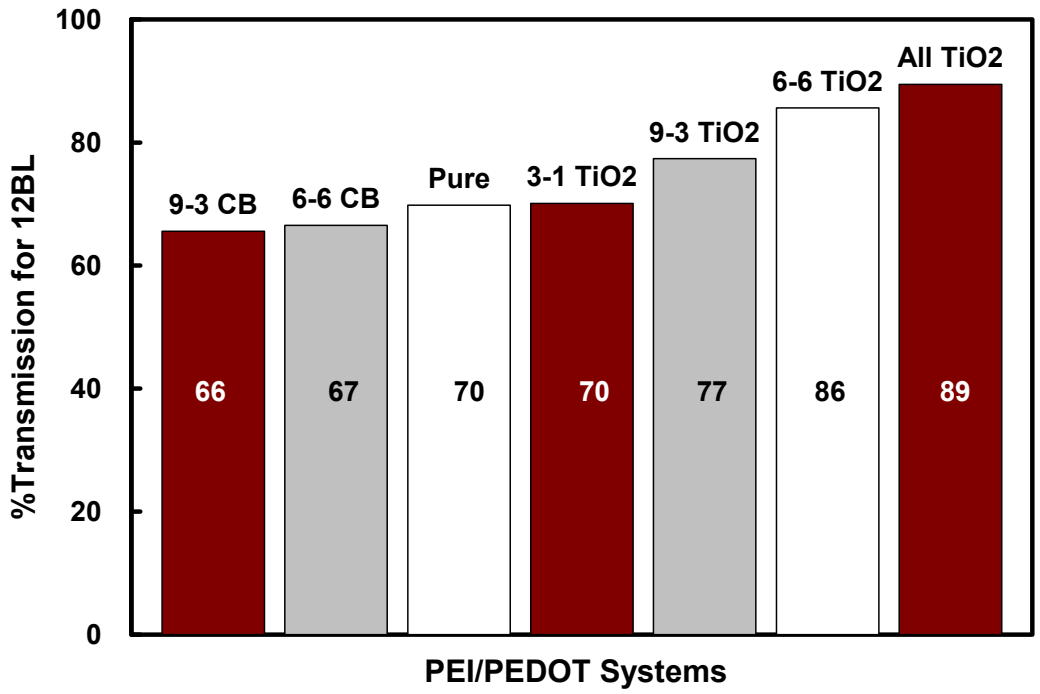

(a)

Figure 21. Transparency of the various systems used for UV protection (a). Transmission values are from 550nm light. Images of some of these films (b) highlight the disparity in %T (b).

(b)

Figure 21. (continued)

Figure 22 shows how film growth changes for the 6-6 CB and 6-6 TiO_2 films when the particle-containing layers replace pure BPEI. The initial growth for 6 bilayers on both films is identical. After the initial 6 bilayers, the film growth rates change dramatically. The TiO_2-containing layers grow very slowly due to the pH of the BPEI + TiO_2 solution being reduced relative to BPEI alone. The carbon black + BPEI layers grow at a much faster rate than the initial 6 bilayers due to the size of the carbon black clusters (100+ nm) that are being deposited. In the case of TiO_2, the 8 nm particles are individual, but the 40nm CB particles exist as covalently-fused clusters. Previous studies have observed large growth rates with BPEI-stabilized CB.[21]

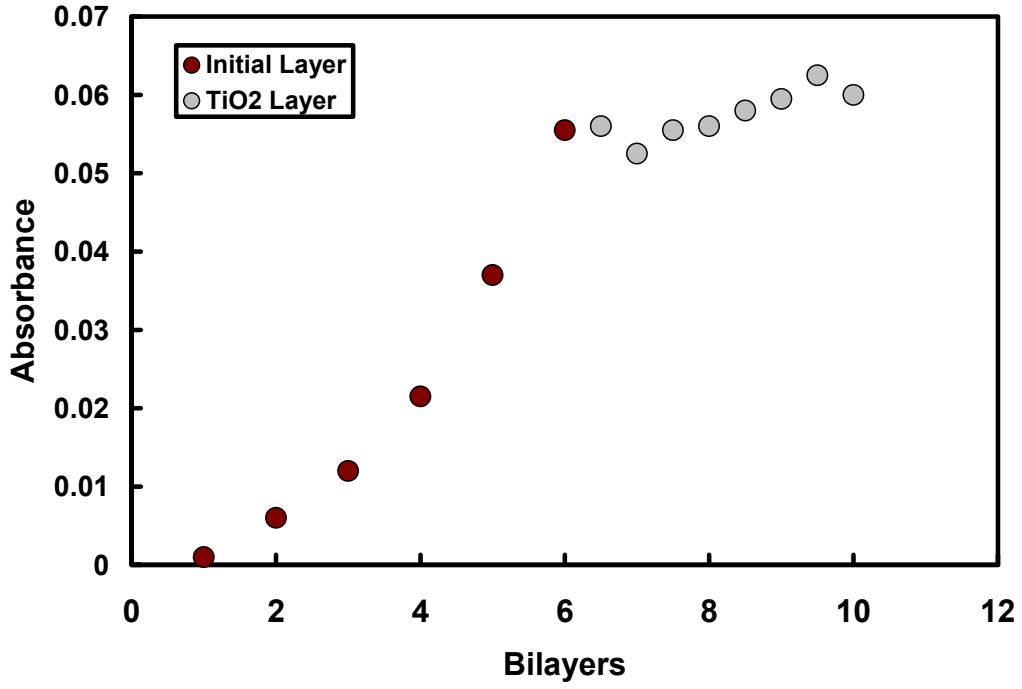

(a)

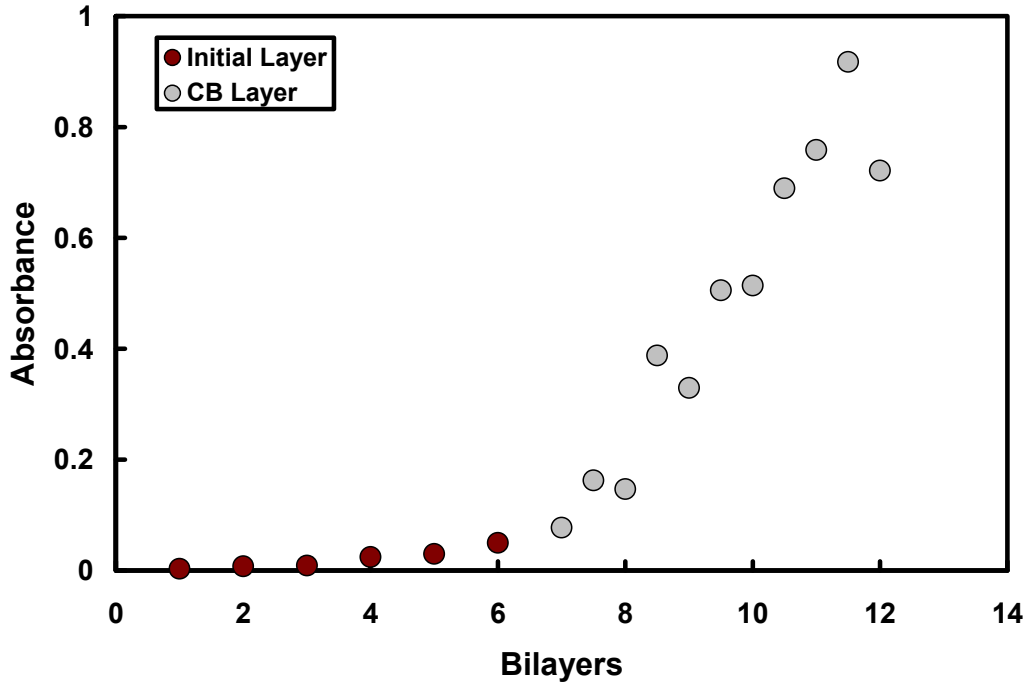

(b)

Figure 22. Absorbance at 550 nm as a function of bilayers deposited for the 6-6 TiO_2 film (a) and the 6-6 CB film (b).

Figure 23 shows the ellipsometric thickness of the 6-6 TiO_2 film. This growth matches the trend seen in the absorbance measurements. For the initial 6 bilayers, the growth rate is approximately 18 nm per bilayer and decreases to 6nm per bilayer for the TiO_2. Based upon the ellipsometry data, the TiO_2 containing thickness is only a quarter of the total film thickness.

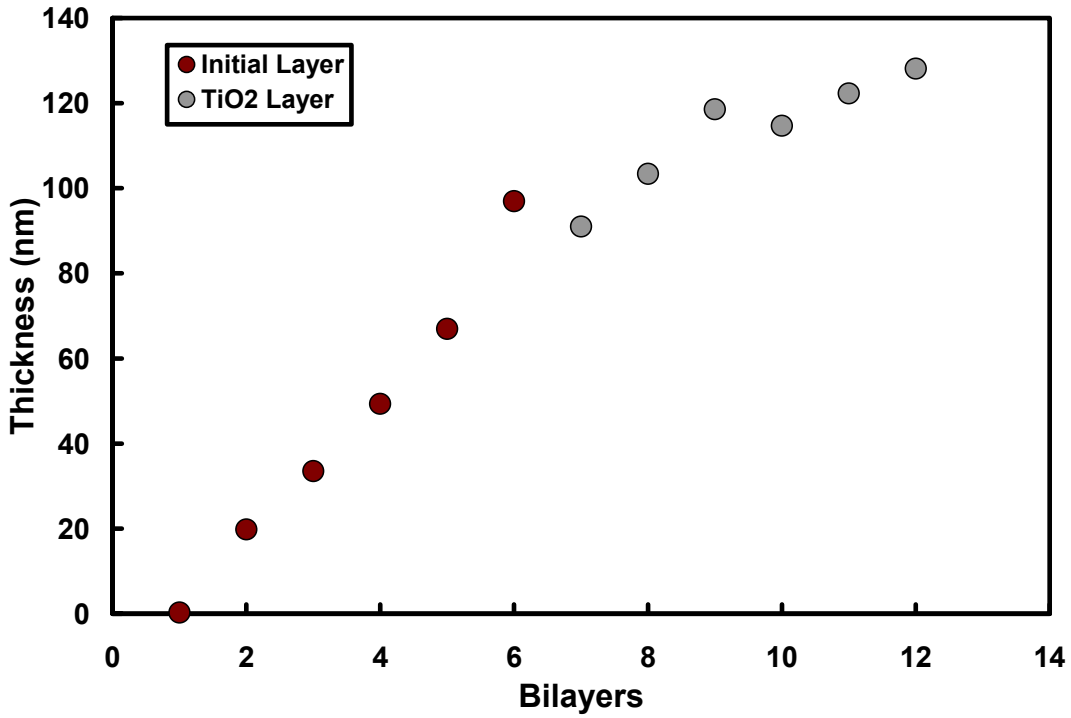

Figure 23. Ellipsometric thickness as a function of bilayers for the 6-6 TiO_2 film.

Figure 24 shows a TEM cross-section of the 6-6 TiO_2 film taken with a JEOL JEM-2010 TEM (JEOL USA, Inc., Peabody, MA). This image confirms the total film thickness measured with ellipsometry, but the TiO_2 section is

approximately half of this thickness. This can be explained by diffusion of TiO_2 into the existing layers already on the substrate and/or smearing of the particles during microtoming.

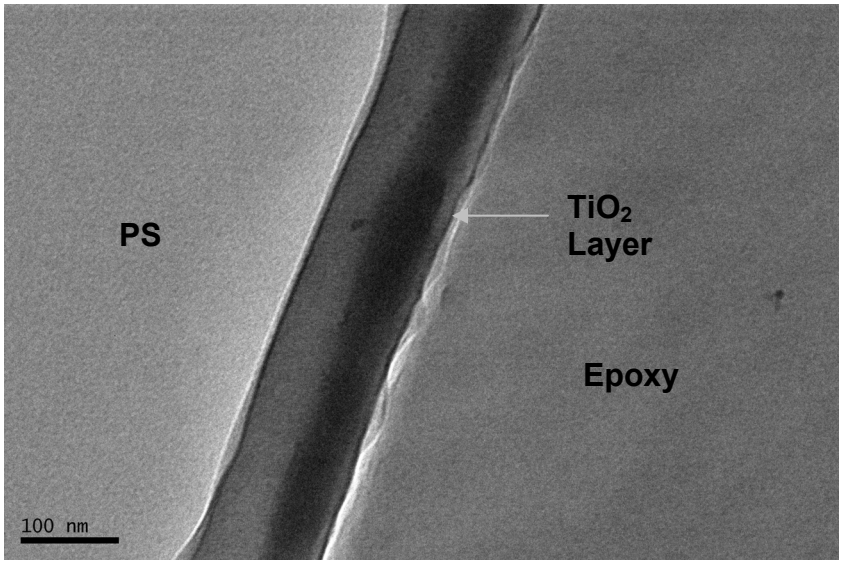

Figure 24. A TEM cross-sectional image of the 12 BL film that highlights the thinner TiO_2-containing portion TEM images of the 6-6 TiO_2 film taken with a and a JEOL JEM-2010.

Conclusion

The addition of UV-absorbing nanoparticles to PEDOT-based thin films was shown to dramatically decrease the degradation of PEDOT electrical conductivity and is a promising approach toward improving its photolytic stability. By adding a 30nm thick (6 BL) TiO_2 containing top section, the film sheet resistance degrades four times slower. Future work will focus on other particles that may absorb UV light, such as colloidal ZnO or carbon nanotubes. The effect of particle size may

also tie into UV protection, along with the location of the particles within these layers. These variables could simultaneously improve stability and transparency.

CHAPTER IV

CONCLUSIONS AND FUTURE WORK

PEDOT was used to create electrically conductive thin films via layer-by-layer assembly. The sheet resistance was tailored by altering both process and compositional variables. As the number of bilayers increased, film thickness increased and sheet resistance decreased. By doping the PEDOT-PSS suspension with 1 wt% DMSO, the conductivity increased by 50 percent with little thickness change for the same number of bilayers deposited. Increasing the charge density of the alternating polycation to 100%, either by altering pH or switching polymers type, decreased the film growth to approximately 6 nm per bilayer, from a maximum of 200 nm per bilayer at 0% charge. The addition of TiO_2 colloids into the LbL process helped to protect the electrical conductivity during UV ageing. 6-6 films (6-bilayers without TiO_2 followed by 6-bilayers with TiO_2) were 1.7 times more conductive than the equivalent carbon black containing films. Additionally, the TiO_2 films were more transparent due to thinner deposition and less aggregation.

Future work with PEDOT could involve creating transparent, flexible, thin film capacitors with PEDOT as the electrode layers and clay (or other nanoparticles) used to make a dielectric layer. Figure 25 shows a schematic of a proposed capacitor made with the layer by layer process. The substrate could be coated with gold (Au) on both ends and a layer of photo-resist could be applied over the gold contacts. Multiple bilayers of a PEDOT-PEI system (PEDOT) could be applied (Step 1 in Fig. 25) and the photo-resist could be removed. New photo-resist would then be added

followed by multiple bilayers of a clay-PEI system (CLAY) (Step 2 in Fig. 25). The photo-resist would then be removed, a new photo-resist added, and the final bilayers of the PEDOT-PEI system would be applied (Step 3 in Fig. 25). Finally, the photo-resist would be removed (Step 4 in Fig. 25) and the capacitor would be fully functional.

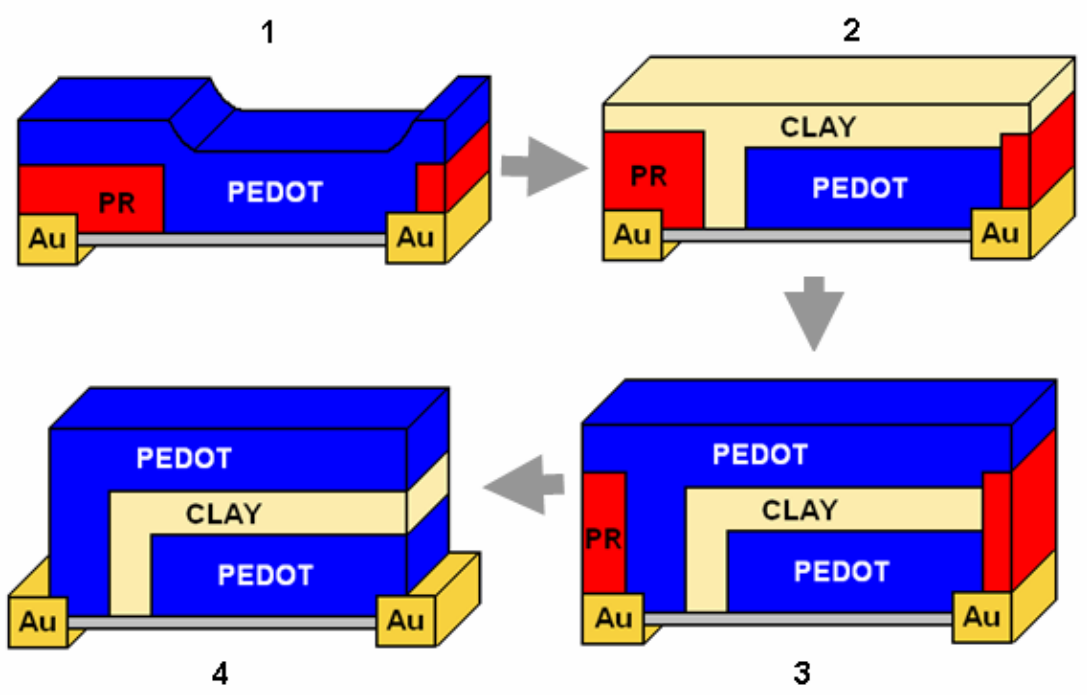

Figure 25. Schematic showing a proposed process to make a capacitor using the LbL process.

The use of magnetic colloids such as γ-Fe_2O_3 (maghemite) and Fe_3O_4 (magnetite) is another area of future work, either in conjunction with or independent of PEDOT. Both materials are multiferroic, meaning they are ferromagnetic and ferroelectric at the same time.[69] This opens new applications in sensors and actuators, where an electric field could be applied to alter the magnetization and vice versa. Preliminary work has been performed on characterization of the growth of

these films. Figure 26 shows TEM images of the Fe_2O_3 and Fe_3O_4 nanoparticles. The particles are somewhat polydisperse, but both the Fe_2O_3 and Fe_3O_4 have diameters less than 25 nm.

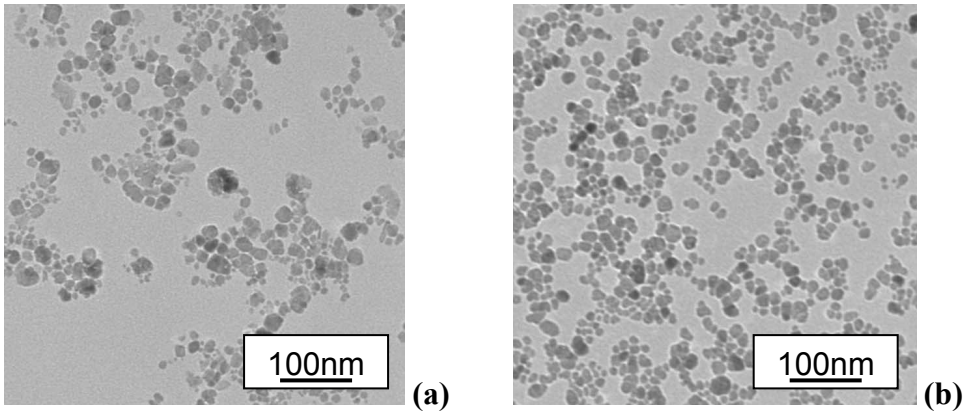

Figure 26. TEM images of Fe_2O_3 (a) and Fe_3O_4 (b) colloidal particles. Images were taken with a JEOL 1200 EX.

Layer-by-layer films were made with aqueous solutions containing 0.2 wt% Fe-based particles alternated with 0.2 wt% LPEI solutions. The Fe_2O_3 particle solutions had a pH of approximately 9.9 while the Fe_3O_4 had a pH of 5.1. Both films exhibit linear growth as shown in Figure 27. The Fe_2O_3 film grows at approximately 2.5 nm per bilayer while the Fe_3O_4 film grows at 22 nm per bilayer. The disparity in film growth can be accounted for by the Fe_3O_4 solution being at a lower pH, causing the stabilizer to be only weakly charged, which causes thicker deposition.

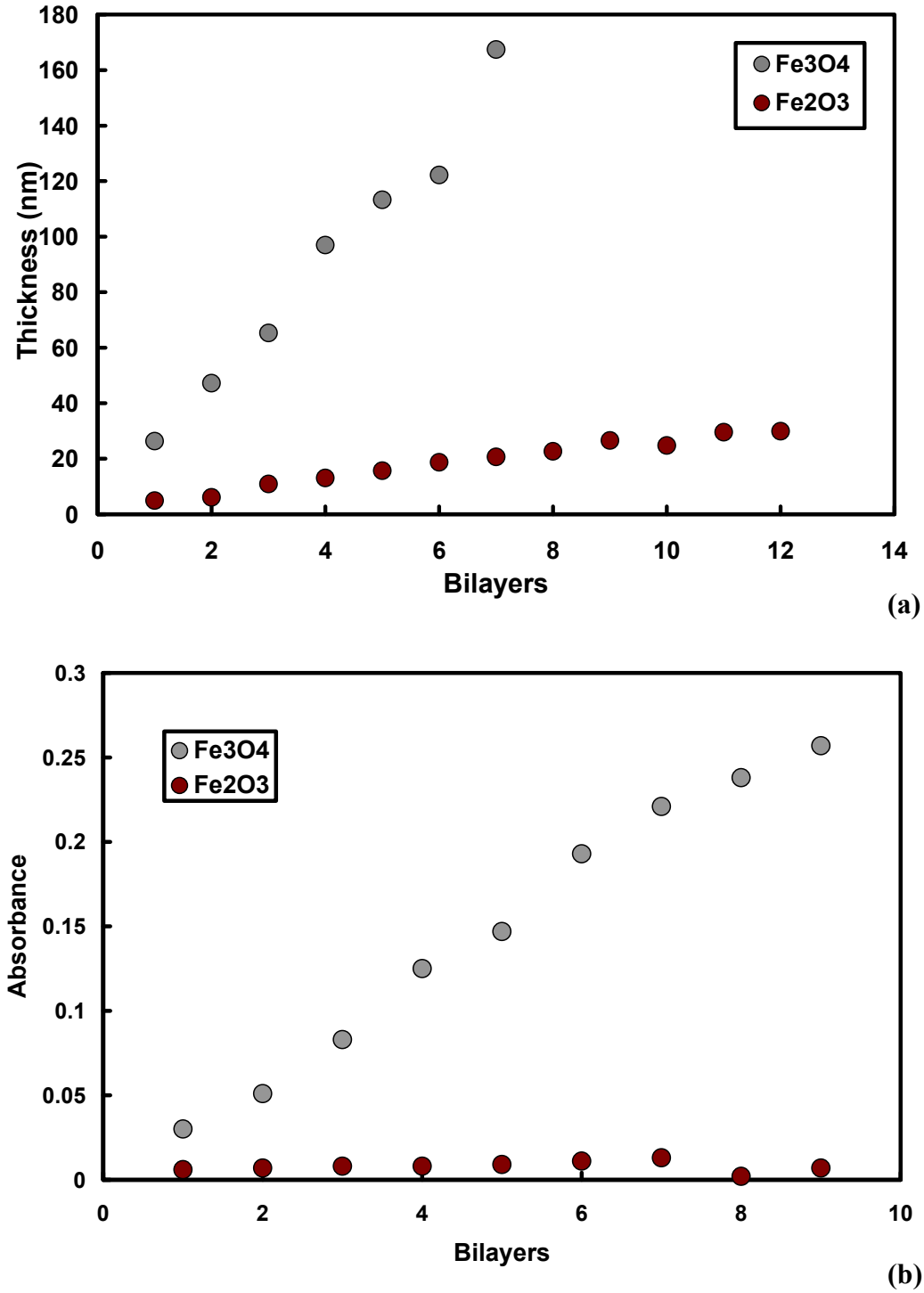

Figure 27. Ellipsometric thickness (a) and absorbance at 550nm (b) as a function of bilayers deposited for the two multiferroic systems.

Further work needs to be performed on tailoring and characterizing the film growth and multiferroic properties of these films. These nanoparticles could be combined with PEDOT-PSS to see if there is a coupling effect. Quantum dots could be added to see if changing a magnetic field would alter their fluorescence characteristics.

REFERENCES

(1) Bertrand, P.; Jonas, A.; Laschewsky, A.; Legras, R. *Macromolecules Rapid Communications* **2000**, *21*, 319-348.

(2) Decher, G.; Lvov, Y.; Schmitt, J. *Thin Solid Films* **1994**, *244*, 772-777.

(3) Lvov, Y.; Decher, G.; Mohwald, H. *Langmuir* **1993**, *9*, 481-486.

(4) Grunlan, J. C.; Choi, J. K.; Lin, A. *Biomacromolecules* **2005**, *6*, 1149-1153.

(5) Fu, J. H.; Ji, J.; Yuan, W. Y.; Shen, J. C. *Biomaterials* **2005**, *26*, 6684-6692.

(6) Rudra, J. S.; Dave, K.; Haynie, D. T. *Journal of Biomaterials Science-Polymer Edition* **2006**, *17*, 1301-1315.

(7) Etienne, O.; Gasnier, C.; Taddei, C.; Voegel, J. C.; Aunis, D.; Schaaf, P.; Metz-Boutigue, M. H.; Bolcato-Bellemin, A. L.; Egles, C. *Biomaterials* **2005**, *26*, 6704-6712.

(8) Ai, H.; Meng, H. D.; Ichinose, I.; Jones, S. A.; Mills, D. K.; Lvov, Y. M.; Qiao, X. X. *Journal of Neuroscience Methods* **2003**, *128*, 1-8.

(9) Yoo, P. J.; Nam, K. T.; Qi, J. F.; Lee, S. K.; Park, J.; Belcher, A. M.; Hammond, P. T. *Nature Materials* **2006**, *5*, 234-240.

(10) Kovtyukhova, N. I.; Ollivier, P. J.; Martin, B. R.; Mallouk, T. E.; Chizhik, S. A.; Buzaneva, E. V.; Gorchinskiy, A. D. *Chemistry of Materials* **1999**, *11*, 771-778.

(11) Kim, H. S.; Sohn, B. H.; Lee, W.; Lee, J.-K.; Choi, S. J.; Kwon, S. J. *Thin Solid Films* **2002**, *419*, 173-177.

(12) DeLongchamp, D. M.; Kastantin, M.; Hammond, P. T. *Chem. Mater.* **2003**, *15*, 1575-1586.

(13) DeLongchamp, D. M.; Hammond, P. T. *Advanced Functional Materials* **2004**, *14*, 224-232.

(14) Hiller, J. A.; Mendelsohn, J. D.; Rubner, M. F. *Nature Materials* **2002**, *1*, 59-63.

(15) Shiratori, S. F. A. S. *Japanese Journal of Applied Physics* **2004**, *43*, 2346-2351.

(16) Roberts, G. G. *Contemporary Physics* **1984**, *25*, 109-128.

(17) Zasadzinski, J. A.; Viswanathan, R.; Madsen, L.; Garnaes, J.; Schwartz, D. K. *Science* **1994**, *263*, 1726-1733.

(18) Iler, R. K. *Journal of Colloid and Interface Science* **1966**, *21*, 569-572.

(19) Ciferri, A. *Supramolecular Polymers*; Marcel Dekker, Inc.: New York, 2000.

(20) Lenahan, K. M.; Wang, Y. X.; Liu, Y. J.; Claus, R. O.; Heflin, J. R.; Marciu, D.; Figura, C. *Advanced Materials* **1998**, *10*, 853-858.

(21) Jan, C. J.; Walton, M. D.; McConnell, E. P.; Jang, W. S.; Kim, Y. S.; Grunlan, J. C. *Carbon* **2006**, *44*, 1974-1981.

(22) Shiratori, S. S.; Rubner, M. F. *Macromolecules* **2000**, *33*, 4213-4219.

(23) Zhang, H. N.; Ruhe, J. *Macromolecules* **2003**, *36*, 6593-6598.

(24) McAloney, R. A.; Sinyor, M.; Dudnik, V.; Goh, M. C. *Langmuir* **2001**, *17*, 6655-6663.

(25) Mermut, O.; Barrett, C. J. *Journal of Physical Chemistry B* **2003**, *107*, 2525-2530.

(26) Sui, Z. J.; Salloum, D.; Schlenoff, J. B. *Langmuir* **2003**, *19*, 2491-2495.

(27) Tan, H. L.; McMurdo, M. J.; Pan, G. Q.; Van Patten, P. G. *Langmuir* **2003**, *19*, 9311-9314.

(28) Lavalle, P.; Gergely, C.; Cuisinier, F. J. G.; Decher, G.; Schaaf, P.; Voegel, J. C.; Picart, C. *Macromolecules* **2002**, *35*, 4458-4465.

(29) Ji, J.; Fu, J. H.; Shen, J. C. *Advanced Materials* **2006**, *18*, 1441-1443.

(30) Schoeler, B.; Poptoschev, E.; Caruso, F. *Macromolecules* **2003**, *36*, 5258-5264.

(31) Kovtyukhova, N.; Ollivier, P. J.; Chizhik, S.; Dubravin, A.; Buzaneva, E.; Gorchinskiy, A.; Marchenko, A.; Smirnova, N. *Thin Solid Films* **1999**, *337*, 166-170.

(32) Paloniemi, H.; Lukkarinen, M.; Aaritalo, T.; Areva, S.; Leiro, J.; Heinonen, M.; Haapakka, K.; Lukkari, J. *Langmuir* **2006**, *22*, 74-83.

(33) Sasaki, T.; Ebina, Y.; Tanaka, T.; Harada, M.; Watanabe, M. *Chemistry of Materials* **2001**, *13*, 4661-4667.

(34) Wang, L. Z.; Ebina, Y.; Takada, K.; Sasaki, T. *Journal of Physical Chemistry B* **2004**, *108*, 4283-4288.

(35) Zeng, T.; Claus, R.; Zhang, F.; Du, W.; Cooper, K. L. *Smart Materials & Structures* **2001**, *10*, 780-785.

(36) Szyszka, B.; Sittinger, V.; Jiang, X.; Hong, R. J.; Werner, W.; Pflug, A.; Ruske, M.; Lopp, A. *Thin Solid Films* **2003**, *442*, 179-183.

(37) DeLongchamp, D. M.; Hammond, P. T. *Advanced Materials* **2001**, *13*, 1455-1459.

(38) Manisankar, P.; Vedhi, C.; Selvanathan, G.; Prabu, H. G. *Journal of Applied Polymer Science* **2007**, *104*, 3285-3291.

(39) Yigitsoy, B.; Varis, S.; Tanyeli, C.; Akhmedov, I. M.; Toppare, L. *Electrochimica Acta* **2007**, *52*, 6561-6568.

(40) Kirchmeyer, S.; Reuter, K. *Journal of Materials Chemistry* **2005**, *15*, 2077-2088.

(41) Heeger, A. J.; Kivelson, S.; Schrieffer, J. R.; Su, W.-P. *Reviews of Modern Physics* **1988**, *60*, 781-850.

(42) Chiang, C. K.; Fincher Jr., C. R.; Park, Y. W.; Heeger, A. J.; Shirakawa, H.; Louis, E. J.; Gao, S. C.; MacDiarmid, A. G. *Physical Review Letters* **1977**, *39*, 1098-1101.

(43) Kirchmeyer, S.; Brassat, L. *Kunststoffe-Plast Europe* **2005**, *95*, 202-208.

(44) Bulut, U.; Cirpan, A. *Synthetic Metals* **2005**, *148*, 65-69.

(45) Choulis, S. A.; Choong, V.-E.; Mathai, M. K.; So, F. *Applied Physics Letters* **2005**, *87,* 113503.

(46) Brewer, P. J.; Lane, P. A.; Huang, J. S.; DeMello, A. J.; Bradley, D. D. C.; DeMello, J. C. *Physical Review B* **2005**, *71*, 125320.

(47) Mabeck, J. T.; DeFranco, J. A.; Bernards, D. A.; Malliaras, G. G.; Hocde, S.; Chase, C. J. *Applied Physics Letters* **2005**, *87*, 013503.

(48) Halik, M.; Klauk, H.; Zschieschang, U.; Kriem, T.; Schmid, G.; Radlik, W.; Wussow, K. *Applied Physics Letters* **2002**, *81*, 289-291.

(49) Hwang, J.; Amy, F.; Kahn, A. *Organic Electronics* **2006**, *7*, 387-396.

(50) Schubert, D. W.; Dunkel, T. *Materials Research Innovations* **2003**, *7*, 314-321.

(51) Newbury, D. E. *Advanced Scanning Electron Microscopy and X-ray Microanalysis*; Springer: New York, 1986.

(52) Tehrani, P.; Kanciurzewska, A.; Crispin, X.; Robinson, N. D.; Fahlman, M.; Berggren, M. *Solid State Ionics* **2007**, *177*, 3521-3527.

(53) Osswald, T. A. *Polymer Processing Fundamentals*; Hanser: Cincinati, 1998.

(54) Donnet, J.-B.; Bansal, R. C.; Wang, M.-J. *Carbon Black: Science and Technology*; CRC Press: Boca Raton, FL, 1993.

(55) Vol. 2007, p Baytron P HC V4 Product Page.

(56) Owens, D. K. *Journal of Applied Polymer Science* **1975**, *19*, 3315-3326.

(57) Zhang, D.; Sun, Q.; Wadsworth, L. C. *Polymer Engineering and Science* **1998**, *38*, 965-970.

(58) Geddes, N. J.; Paschinger, E. M.; Furlong, D. N.; Caruso, F.; Hoffmann, C. L.; Rabolt, J. F. *Thin Solid Films* **1995**, *260*, 192-199.

(59) Jang, W. S.; Grunlan, J. C. *Review of Scientific Instruments* **2005**, *76*, 103904.

(60) Crispin, X.; Marciniak, S.; Osikowicz, W.; Zotti, G.; Van der Gon, A. W. D.; Louwet, F.; Fahlman, M.; Groenendaal, L.; De Schryver, F.; Salaneck, W. R. *Journal of Polymer Science Part B-Polymer Physics* **2003**, *41*, 2561-2583.

(61) Tang, Z. X.; Donohoe, S. T.; Robinson, J. A.; Chiarelli, P. A.; Wang, H. L. *Polymer* **2005**, *46*, 9043-9052.

(62) Ladam, G.; Schaad, P.; Voegel, J. C.; Schaaf, P.; Decher, G.; Cuisinier, F. *Langmuir* **2000**, *16*, 1249-1255.

(63) Granlund, T.; Pettersson, L. A. A.; Anderson, M. R.; Inganas, O. *Journal of Applied Physics* **1997**, *81*, 8097-8104.

(64) Cho, J.; Char, K.; Kim, S. Y.; Hong, J. D.; Kim, D. Y.; Lee, K. B. *Synthetic Metals* **2001**, *124*, 415-419.

(65) Smith, R. R.; Smith, A. P.; Stricker, J. T.; Taylor, B. E.; Durstock, M. F. *Macromolecules* **2006**, *39*, 6071-6074.

(66) Orata, D.; Buttry, D. A. *Journal of the American Chemical Society* **1987**, *109*, 3574-3581.

(67) Tada, K.; Onoda, M. *Journal of Physics D-Applied Physics* **2002**, *35*, 192-195.

(68) Heywang, G.; Jonas, F. *Advanced Materials* **1992**, *4*, 116-118.

(69) Cai, N.; Zhai, J.; Nan, C. W.; Lin, Y.; Shi, Z. *Physical Review B* **2003**, *68*, 224103.

VITA

Name:	Thomas James Dawidczyk
Address:	31 West Applewood Drive, Charlton, MA 01507
Email Address:	TDawidczyk@gmail.com
Education:	B.S., Mechanical Engineering, The University of Massachusetts at Amherst, 2003
	M.S., Mechanical Engineering, Texas A&M University, 2008